

國立臺灣大學醫學院微生物學科暨研究所



碩士論文

Graduate Institute of Microbiology

College of Medicine

National Taiwan University

Master Thesis

NRIP 藉由調控 F-actin 參與肌細胞融合

NRIP regulates F-actin for myoblast fusion

韓雅如

Ya-Ju Han

指導教授：陳小梨 博士

Advisor: Show-Li Chen, Ph.D.

中華民國 108 年 7 月

July 2019

國立臺灣大學 (碩) 博士學位論文
口試委員會審定書

中文題目：NRIP 藉由調控 F-actin 參與肌細胞融合

英文題目：NRIP regulates F-actin for myoblast fusion

本論文係 韓雅如 君 (學號 R06445109) 在國立臺灣大學微生物學所完成之碩 (博) 士學位論文，於民國 108 年 07 月 23 日承下列考試委員審查通過及口試及格，特此證明

口試委員：

陳川梨

(簽名)

(指導教授)

翁雅雯

曾香如

蔡力凱

蔡錦華

系主任、所長

(簽名)


致謝

兩年的碩士生涯轉眼間就到了尾聲，這段求學過程中我遇到了一群很棒的、值得我一生學習的人們。首先，非常謝謝指導教授 陳小梨老師細心、嚴謹的教導，謝謝老師平時對我在邏輯上的訓練以及實驗上提供許多學習機會，在老師身上，我學到了對於求知的熱情及毅力，以及保有自我核心價值的重要性。除此之外，也非常感謝我的三位口試委員蔡力凱醫師、曾秀如老師及劉雅雯老師在進度報告中無私地給予我寶貴的建議，點出我忽略及該注意的問題，讓我能夠更精進自己。

另外也很感謝男神信雄學長，學長不僅常在實驗上給我精闢的建議，平時也常關心我們的近況，督促我要多出去踏青、和吱吱吃飯，更重要的是在學長身上學到豁達的人生態度，怎麼調適遭遇失敗時的心態，哪些人、事對自己才是重要的，學長不只是實驗上的專家，也是厲害的心靈導師。楚歲學長經常跟我分享實驗室的大小事，讓我可以比較快進入狀況，懷念碩一時坐在隔壁的垃圾話時光，學長在實驗上的巧手及細心是我學習的目標，學長的幽默也為實驗室帶來很多歡樂，祝福你在美國一切順利。還有最喜歡的野蠻人們，謝謝最暖的伯翰，總是替別人付出很多，很暖的關心大家，讓實驗室氣氛變得很好，謝謝你罩了我跟吱吱兩年，真的是無限的感謝！還有首領詩浩，每次都默默觀察並在關鍵時刻神救援，在你身上看到了豁達的處世態度，但同時又能把事情都做好，真心佩服。認識了六年的婉欣，大學時都不知道你是女神般的存在，能力超好但很謙虛，也很樂觀，包容我剛進實驗室時問的很多蠢問題，聽到你的笑聲就覺得很溫暖，捶桌更棒！還有做事效率超高的韻心，碩一時一直把你當成目標，每次做實驗前總是先做好準備、計畫好一切，然後再俐落的解決每件事，給人很可靠的感覺。想念碩一時大家一起討論實驗、互相幫忙解決問題，天南地北聊天大笑的時光，也祝福你們在工作上一切順利！另外也很感謝我的同伴吱吱，謝謝很暖的你在這兩年來大大小小各種的幫忙，不管是在實驗上、生活上還有我申請交換學生時，總是不斷鼓勵很容易焦慮的我，也時常在我覺得很多事做不完時自願幫我分擔，但其實你身上的事並沒有比較少，你總是這麼善良溫暖又熱心，聽到你的大笑聲就覺得超療癒，能和你在同間實驗室當同學真的是我這輩子的福氣！另外也很感謝碩一的小朋友們，短短一年，在你們身上我也學到一些我沒有的特質，謝謝熱心、無所不能的翔翔提醒我要準時吃飯、學我各種聲音，你絕對是科學家的料；為實驗室帶來歡樂、思慮縝密、活潑的婉恩；貼心聰明、個性可愛的亦欣；精明能幹、手很巧的釗昕，還有默默關心著大家，脾氣很好的皓文，祝福你們實驗順利。

最後最感謝我最棒的家人，總是對我無比的包容和體諒，給我滿滿的鼓勵及作為我最強的後盾，支持著我想做的事，謝謝你們體諒我做實驗很少回家，經常大老遠上來台北找我，煮家鄉味給我吃，外食這麼多年，最喜歡吃的就是你們煮的菜，能讓你們驕傲是我最開心的事，也會一直努力做到，最愛你們了！另外也很感謝一直陪在身邊的慶輔，在我壓力大時拉著我去運動、吃美食，總在你身上得到滿滿的正能量。最後謝謝碩士班幫助過我的所有人，短短一頁的致謝無法表達我對這段期間認識的人的感謝及喜愛，期待之後再見，謝謝你們！

中文摘要



核受體結合蛋白(Nuclear receptor interaction protein, NRIP)又名 IQWD1 或 DCAF6，是一個鈣離子依賴性的攜鈣素(calmodulin)結合蛋白，NRIP 由 860 個胺基酸所組成，其中包含七個 WD 40 repeats 及一個 IQ motif。在本實驗室先前的研究中，我們發現在注射心臟毒素(cardiotoxin)造成肌肉受損所產生的肌肉再生中，全身性 NRIP 基因剔除鼠與正常小鼠相比，會產生較高比例的小尺寸的肌纖維(myofiber)，顯示 NRIP 可能會調控肌細胞融合(myoblast fusion)。先前已有許多研究指出肌細胞的融合與肌動蛋白結合蛋白(actin-binding protein)所調控之肌動蛋白細胞骨架重塑有密切關係。此外，我們實驗室先前的研究發現在 *in vitro* 的情況下，NRIP 和肌動蛋白有交互作用，因此在本篇實驗中我們進一步探討 NRIP 是否會藉由調控肌動蛋白參與在肌細胞融合中。

首先，利用細胞的免疫沉澱法(immunoprecipitation)我們確認在 *in vivo* 的情況下，NRIP 和肌動蛋白彼此間也會有交互作用；除了肌動蛋白結合蛋白以外，許多膜蛋白也被報導會促進肌細胞的融合，因此我們做了細胞質、膜蛋白分離的實驗，並發現 NRIP 分布在細胞核及質中的比例是差不多的。

接著，我們進一步探討 NRIP 是否會調控肌小管形成(myotube formation)，利用 NRIP 基因剔除肌細胞 KO19，我們發現與正常肌細胞 C2C12 比起來，KO19 形成肌小管的能力嚴重受損，並伴隨著肌細胞分化及融合能力的下降，顯示 NRIP 確實會調控肌小管形成，接著我們進一步在 C2C12 及 KO19 中大量送入 NRIP，發現不管在 C2C12 或 KO19 中，外送 NRIP 皆能促進肌小管的形成。

在肌細胞融合過程中，由肌動蛋白所構成類似足體的構造(podosome-like structure)對於融合孔的產生是重要的，首先我們觀察到 NRIP 會聚集在肌細胞接合處，顯示 NRIP 確實可能會調控肌細胞融合，接著我們利用顯微影像曠時攝影技術(time-lapse microscopy)觀察到 NRIP 與肌動蛋白共定位(colocalize)且聚集在細胞質中形成焦點並往細胞膜外突出形成類似足體的構造，顯示其可能參與在肌細胞融

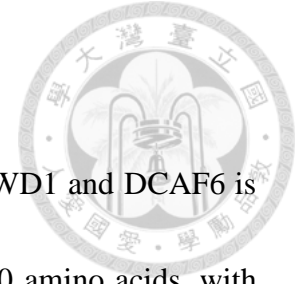
合侵入的過程中。

此外我們利用不同 NRIP 的片段探討 NRIP 的哪一段會和肌動蛋白結合，結果發現 NRIP 可能會透過 WD67 直接與肌動蛋白連結，或是利用 IQ motif 間接經由輔肌動蛋白異構體(α -actinin2, ACTN2)與肌動蛋白連結，我們並進一步探討 NRIP 與肌動蛋白連結是否與肌細胞融合有關，結果顯示在 KO19 中大量送入 WD67 可以促進肌細胞融合，代表 NRIP 與肌動蛋白連結與肌細胞融合是有關連的。

最後，我們探討了由 NRIP 所調控之肌細胞生成素(myogenin)主導的肌小管形成，我們先前的研究結果顯示 NRIP 藉由與調鈣素結合，活化下游鈣調磷酸酶(calcineurin)及鈣調蛋白肌酶 II (calmodulin kinase II)進而促進肌細胞生成素的表現，我們進一步將 C2C12 中 NRIP 基因減弱(gene knockdown)，發現肌細胞生成素及肌球蛋白重鏈(myosin heavy chain)的 RNA 及蛋白質表現皆較控制組下降，表示 NRIP 會經由調控肌細胞生成素參與在肌小管形成中。總體來說，我們發現了 NRIP 可以透過和肌動蛋白結合進而去調控肌細胞融合外，也可以透過調控肌細胞生成素參與在肌小管形成的過程中。

關鍵詞:核受體結合蛋白、肌動蛋白、肌細胞融合、肌細胞生成素、WD40 repeats

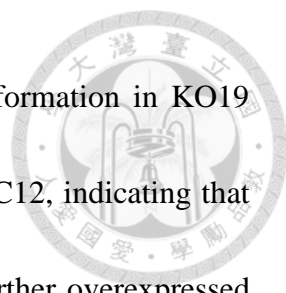
Abstract



Nuclear receptor interaction protein (NRIP) also named as IQWD1 and DCAF6 is a Ca^{2+} -dependent calmodulin-binding protein. NRIP consists of 860 amino acids, with seven WD40 repeats and one IQ motif. In previous study, we observe that NRIP global knockout (gKO) mice show higher frequency of small myofiber size distribution than wild-type mice at day 21 post cardiotoxin-induced injury during muscle regeneration, indicating that NRIP may regulate myoblast fusion to form myofiber. Myoblast fusion has been reported to be strongly associated with actin cytoskeleton remodeled by actin-binding proteins. Moreover, our unpublished results reveal that NRIP can interact with F-actin *in vitro*. Therefore, in this study, we investigated whether NRIP through interacting with actin to regulate myoblast fusion during myogenesis.

First, we investigated whether NRIP interacts with actin *in vivo*. By performing immunoprecipitation assay, the results revealed that NRIP and actin interacted reciprocally *in vivo*. Not only actin-binding proteins but also membrane-bound proteins have been reported to promote myoblast fusion. Therefore, we next performed cytosolic and membrane protein fractionation and found that NRIP expressed in both cytoplasm and membrane with nearly equal amount.


Next, we examined whether NRIP is responsible for myotube formation. We generated NRIP-null C2C12 myoblast—KO19. By conducted immunofluorescence



assay, we observed the severely impaired the ability of myotube formation in KO19 with both reduced differentiation and fusion index compared to C2C12, indicating that NRIP is responsible for myoblast differentiation and fusion. We further overexpressed NRIP in C2C12, and the results showed that NRIP can enhance the ability of myotube formation in C2C12. Moreover, overexpression of NRIP in KO19 could rescue myotube formation. These results indicate that NRIP is responsible for myotube formation.

During myoblast fusion, the F-actin-enriched podosome-like structure is essential for fusion pore formation. We first observed that NRIP concentrated at the site of cell-cell contact, implying that NRIP may play a role in fusion. Next, we performed time-lapse microscopy and discovered that NRIP and actin colocalized and concentrated to form NRIP- and actin-enriched foci in cytoplasm and then protruded toward cell membrane to form podosome-like structure which might promote invasion during myoblast fusion. We also performed cell fusion assay and verified that NRIP could enhance myoblast fusion.

Realizing NRIP is an actin-binding protein, we further investigate which domain of NRIP is responsible for binding with actin. We performed immunoprecipitation assay and the results suggested that NRIP might directly interact with actin through WD67 domain and indirectly bind with actin through IQ motif in an ACTN2-dependent manner. To examine whether NRIP binding with actin is correlated with myoblast fusion, we



overexpressed WD67 domains which can bind with actin in KO19 and examined myotube formation. The fusion index was significantly higher in KO19/WD67 than KO19/vector, indicating that the WD67 domain of NRIP binding with actin is correlated to myoblast fusion.

Apart from NRIP-regulated actin for myotube formation, we also investigated NRIP-regulated myogenin for myotube formation. Our unpublished results reveal that NRIP regulates myogenin through binding with Calmodulin (CaM) to activate calcineurin (CaN) and calmodulin kinase II (CaMKII) signaling pathway. We further performed Ad-shNRIP to knockdown C2C12 during myogenesis, and found that the protein and RNA expression levels of myogenin and MyHC decreased, suggesting that NRIP also through myogenin to regulate myotube formation. Collectively, NRIP not only acts through interacting with actin to regulate myoblast fusion but also through regulating myogenin to take part in myotube formation.

Key words: NRIP, actin, myoblast fusion, myogenin, WD40 repeats

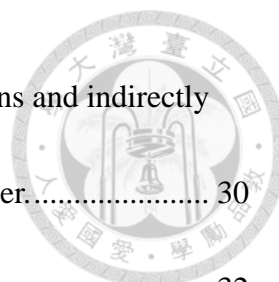
目錄



口試委員會審定書	I
致謝	II
中文摘要	III
Abstract.....	V
目錄	VIII
Chapter 1 Introduction.....	1
1.1 Characteristics of Nuclear receptor interaction protein (NRIP)	1
1.2 The role of NRIP in muscle function.....	2
1.3 The mechanism of myoblast fusion during myogenesis	4
1.4 Actin binding proteins for myoblast fusion	6
1.5 The characteristics and functions of WD40 domain.....	8
1.6 Membrane-bound proteins for myoblast fusion	10
1.7 Aims of the study.....	12
Chapter 2 Materials and methods	14
2.1 Generation of NRIP-knockout cell line--KO19	14
2.2 Cell culture and transfection.....	15
2.3 Western blots analysis.....	15
2.4 Cytosolic and membrane protein fractionation	16



2.5 RNA extraction and RT-PCR.....	17
2.6 Immunoprecipitation assay.....	17
2.7 Immunofluorescence staining.....	18
2.8 Cell fusion assay.....	19
2.9 Time-lapse microscopy.....	19
2.10 Recombinant adenovirus generation and infection	19
2.11 Site-directed mutagenesis	20
2.12 Statistical analysis	21
Chapter 3 Results.....	22
3.1 NRIP reciprocally interacts with actin <i>in vivo</i>	22
3.2 NRIP is localized in nucleus, cytoplasm and plasma membrane in C2C12 cells.	23
3.3 NRIP is responsible for myotube formation.....	24
3.4 Overexpression of NRIP in C2C12 enhances the ability of myotube formation.	25
3.5 NRIP can rescue myotube formation in NRIP-null KO19 cells.....	26
3.6 NRIP concentrates at the site of fusion and interacts with actin to form podosome-like structure.	27
3.7 NRIP promotes myoblast fusion.....	29



3.8 NRIP may directly interact with actin through WD67 domains and indirectly bind with actin through IQ motif in an ACTN2-dependent manner.....	30
3.9 The WD67 domains of NRIP are related to myotube formation.	32
3.10 Knockdown of NRIP down-regulates the RNA and protein expression levels of myogenin and MyHC during C2C12 differentiation.	33
Chapter 4 Discussion.....	36
Chapter 5 Figures	46
Chapter 6 Supplementary information	62
Chapter 7 Appendix.....	68
Chapter 8 References.....	70

Chapter 1

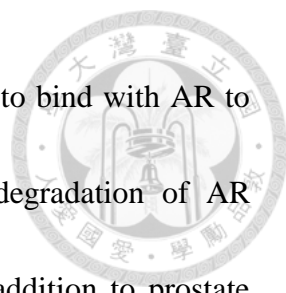
Introduction



1.1 Characteristics of Nuclear receptor interaction protein (NRIP)

Nuclear receptor interaction protein (NRIP) is also known as DCAF6 and IQWD1, consisting of 860 amino acids, with seven WD40 repeats and one IQ motif (Chang et al., 2011; Tsai et al., 2005). NRIP was firstly discovered as an androgen receptor (AR)-interaction protein by using yeast two-hybrid system. NRIP was also found to enhance the transcription activity of AR and GR-driven genes in the presence of AR and GR ligands. Knockdown of NRIP diminishes cell proliferation in prostate (LNCaP) and cervical (C33A) cancer cells (Tsai et al., 2005). Besides, NRIP is an AR-target gene, which can enhance its own expression through forming a complex with AR to protect AR protein from proteasome degradation (Chen et al., 2008). Our previous study shows that NRIP can stabilize HPV-16 E2 protein and induce HPV gene expression. NRIP can directly bind with calmodulin (CaM) through its IQ motif in the presence of Ca^{2+} , and thus activate the phosphatase calcineurin (CaN) to dephosphorylate E2 to prevent polyubiquitination and degradation of E2, enhancing E2 protein stability and E2-driven protein expression (Chang et al., 2011).

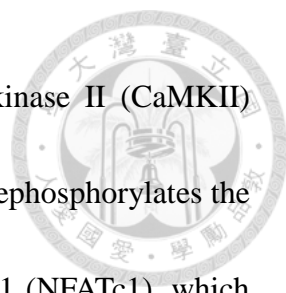
Moreover, NRIP is related to human cancers. According to our previous study, the expression levels of NRIP and AR are higher in prostates cancer tissue than in



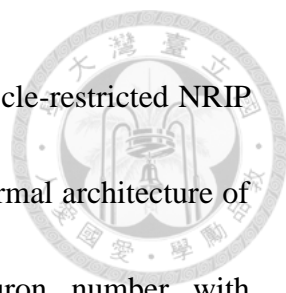
non-neoplastic controls. It is found that NRIP compete with DDB2 to bind with AR to stabilize AR by decreasing DDB2-mediated ubiquitination and degradation of AR through CUL4-DDB1 E3 ligase complex (Chen et al., 2017). In addition to prostate cancer, NRIP expression is found in six human malignancies, including esophageal, colon, breast, ovarian, skin and pancreatic cancers (Han et al., 2008). In terms of other diseases associated with NRIP, from genetic studies by analyzing single nucleotide polymorphism (SNP), genetic variations in NRIP genome location [Chr1q24.2; NC_000001.10(167905797..168045081)] are associated with cardiovascular disease, osteoporosis and schizophrenia (Cheung et al., 2009; Ehret et al., 2009; Shi et al., 2011). Recently, *NRIP (IQWD1)* RNA expression has been reported to be lower in dystrophic muscles than normal muscles in limb-girdle muscular dystrophy (LGMD) patients (Zhang et al., 2006). Collectively, NRIP is involved in not only human cancers but several diseases.

1.2 The role of NRIP in muscle function

By generating global NRIP-knockout (gKO) mice, it is found that NRIP-gKO mice display reduced muscle strength, susceptibility to fatigue and impaired adaptive exercise performance (Chen et al., 2015). The mechanisms of NRIP-regulated muscle contractility is that in the presence of Ca^{2+} , NRIP can bind with CaM through its IQ



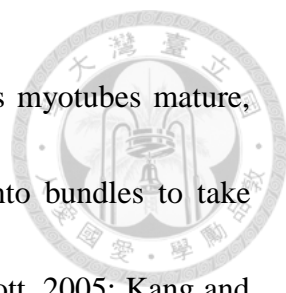
motif to activate downstream phosphatase CaN and calmodulin kinase II (CaMKII) (Bahler and Rhoads, 2002; Chang et al., 2011). The activated CaN dephosphorylates the transcription factor nuclear factor of activated T-cells, cytoplasmic 1 (NFATc1), which then translocates to nucleus to trigger the expression of a subset of genes, such as type-I slow myosin to induce muscle-fiber-type switch towards a slow-twitch and oxidative type for sustained muscle activity. In addition to CaN, NRIP together with CaM can also stimulate the phosphorylation of CaMKII to activate it, resulting in the regulation of Ca^{2+} homeostasis through releasing Ca^{2+} to cytoplasmic and uptake internal Ca^{2+} to sarcoplasmic reticulum (SR) to regulate muscle contraction (Chen et al., 2015). Furthermore, NRIP-regulated CaN and CaMKII has been reported to participate in muscle regeneration which involves in myogenesis. (Abraham and Shaw, 2006; Chen et al., 2015; Demonbreun et al., 2010). Myogenin and embryonic MyHC (eMyHC; MYH3) are markers of myogenesis and myotube formation (Bassel-Duby and Olson, 2006). Our previous study demonstrates that the RNA expression levels of myogenin and eMyHC are significant lower in NRIP-gKO mice than in wild-type mice at day 6 after injury during cardiotoxin-induced muscle regeneration (Chen et al., 2015). Skeletal myofibers form by fusion of myoblasts to produce multinucleated myotubes (Chal and Pourquie, 2017). NRIP-gKO mice have a significant higher proportion of small-sized myofiber than wild-type mice at day 21 post injury (Chen et al., 2015). Thus, NRIP may have a



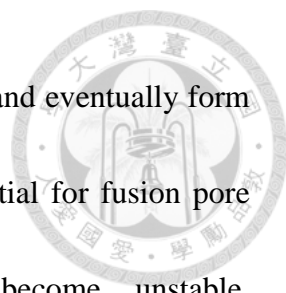
role in myoblast fusion. Recently, our investigation reveals that muscle-restricted NRIP knockout (cKO) mice display motor neuron degeneration with abnormal architecture of neuromuscular junction (NMJ) shown by reduced motor neuron number with small-sized neuron in lumbar spinal cord as well as denervating change and decreased myonuclei at NMJ in skeletal muscles. The underlying mechanism reveals that myogenin may be the candidate. NRIP and myogenin are colocalized around acetylcholine receptors at NMJ, and NRIP-cKO mice are found to perform lower RNA expression of myogenin at synaptic region than wild-type mice. Hence NRIP maintain NMJ integrity via regulating myogenin expression (Chen et al., 2018). Given above, NRIP not only regulates muscle contraction and regeneration but also stabilize NMJ and prevent motor neuron death. Furthermore, NRIP are found to regulate myogenin, eMyHC and affect myofiber size during muscle regeneration, implying that NRIP may participate in myogenesis and myoblast fusion.

1.3 The mechanism of myoblast fusion during myogenesis

Myogenesis is the process of developing skeletal muscle during embryonic development and regeneration after injury. In the beginning, myogenic progenitor cells are activated from quiescence to become myoblasts, followed by proliferation and differentiation of myoblasts into myocytes and exit from cell cycle. These differentiated



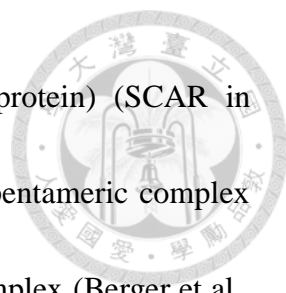
myocytes then fuse together to form a multinucleated myotube. As myotubes mature, they undergo secondary fusion to form myofibers which group into bundles to take shape of skeletal muscle (Bentzinger et al., 2012; Berkes and Tapscott, 2005; Kang and Krauss, 2010; Knight and Kothary, 2011). Myoblast fusion plays a fundamental role in forming a nucleated syncytium to have muscle function. In mice, first, myoblasts migrate extensively prior to fusion, consistent with the expression of receptors for chemokines, growth factors and other molecules, followed by recognition and adhesion between myoblasts mediated by adhesion molecules, such as immunoglobulin (Ig) superfamily, integrins and cadherins, and muscle cell will extent actin-based lamellipodium and filopodium to recognize and adhere to contact neighboring muscle cells. Next, two fusion partners rearrange actin cytoskeleton to form F-actin-enriched invasive podosome-like structure (PLS) for invasion. Many actin polymerization and binding proteins are important for actin remodeling to form the actin-enriched protrusive podosome-like structure. In *Drosophila*, myoblast fusion occurs in two types of cells, founder cells and fusion competent myoblasts (FCMs), which are specified by the expression of transcription factors (Chen and Olson, 2004; Tixier et al., 2010). A FCM is attracted by a founder cell for fusion. However, it is still a no definitive question about whether vertebrates possess FCMs and founder cells (Powell and Wright, 2012). Once the myoblast membranes are brought into close proximity by actin protrusion



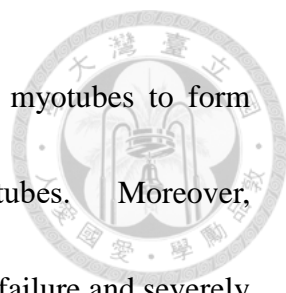
invading into the fusion partner, the lipid bilayers become unstable and eventually form the fusion pore. At this time, the podosome-like structure is essential for fusion pore formation (Sens et al., 2010). When cell membranes become unstable, phosphatidylserine (PS) transiently expose to cell surface, which further recognized by the cell surface PS receptors, such as BAI family and stabilin-2. The binding of PS by PS receptors has been reported to promote myoblast fusion, while studies have not yet to identify any molecule to facilitate this step in *Drosophila*. (Bernadzki et al., 2014; Hamoud et al., 2014; Hochreiter-Hufford et al., 2013; Park et al., 2016; Sens et al., 2010). Finally, the formation of fusion pores leads to fusing of myoblasts to form a multinucleated myotube (Abmayr and Pavlath, 2012; Kim et al., 2015).

1.4 Actin binding proteins for myoblast fusion

Several actin binding proteins functioning in actin cytoskeleton remodeling are important for myoblast fusion, not only by facilitating the formation of actin-based protrusion but also by helping actin polymerization to provide a positional cue for prefusion vesicles transport (Kim et al., 2007; Nowak et al., 2009; Richardson et al., 2007). Among them, actin-related protein 2/3 (Arp2/3) complex functions for actin polymerization. Through binding to pre-existing actin filaments, Arp2/3 complex promotes the formation of new actin filaments by branching. SCAR (suppressor of




cAMP activator) /WAVE (WASP family verprolin homologous protein) (SCAR in *Drosophila*; WAVE in vertebrates) actin remodeling complex is a pentameric complex that promotes actin polymerization through activation of Arp2/3 complex (Berger et al., 2008). It has been reported that either *SCAR* or *Arp3* loss-of-function mutants in *Drosophila* reveal a moderate myoblast fusion defect with the enlarged actin foci, which suggests the impaired actin reorganization for its dissolution. Hence, the actin binding protein SCAR and Arp2/3 are crucial for myoblast fusion (Richardson et al., 2007). Besides, the Nck-associated protein 1 (Nap1), a vertebrate ortholog of the *Drosophila* fusion protein Kette, is a member of WAVE actin remodeling complex, and is a cytosolic actin-binding protein (Bogdan and Klambt, 2003). Previous study demonstrates that knockdown of Nap1 by *Nap1*-shRNA inhibit myoblast fusion and myotube formation. The fusion index is significant lower in Nap1-knockdown myoblasts compared to control group. Nap1-knockdown myoblasts also show longer average lifetime of F-actin aggregates, revealing the abnormal behaviors of actin reorganization during myoblast fusion (Nowak et al., 2009). Moreover, FilaminC is a muscle-specific actin-binding protein which crosslinks actin filament into orthogonal networks (Hartwig and Stossel, 1975). FilaminC mainly localizes to Z-disc of the sarcomere, and can also be found in the sarcolemma of muscles in a low amount (Thompson et al., 2000; van der Ven et al., 2000). Knockdown of FilaminC in C2C12 myoblast by siRNA displays



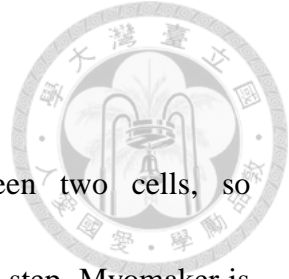
defects in both differentiation and fusion ability with collapse of myotubes to form multinucleated “myoballs” rather than elongated myotubes. Moreover, FilaminC-deficient mice die shortly after birth due to the respiratory failure and severely reduced body weight with decreased number of muscle fibers, indicating defects in differentiation and myoblast fusion (Dalkilic et al., 2006). Collectively, in terms of actin-binding proteins, either functioning in actin polymerization or in actin crosslinking has been reported to play an important role in myoblast fusion.

1.5 The characteristics and functions of WD40 domain

The WD40 repeat is a short structural motif that consists of approximately 40 amino acids with a glycine-histidine (GH) dipeptide 11 to 24 residues from its N-terminus and terminating in a tryptophan-aspartic acid (WD) dipeptide. WD40 domain-containing proteins have 4 to 16 repeats and have been reported to form a circular seven β -propeller structure. The WD40 domain consists of several repeats, a variable region of about 11 to 20 residues at the beginning and followed by a more common repeats of residues. These repeats typically form a four stranded anti-parallel β -sheet or blade. These blades come together to form a multi-bladed β -propeller structure with nearly all of them containing seven blades (Li and Roberts, 2001; Smith et al., 1999). WD40-containing proteins have been reported to participate in several



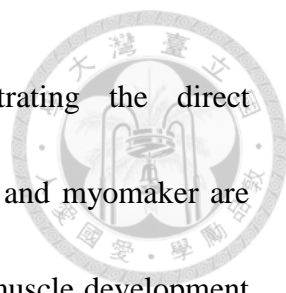
biological functions including actin cytoskeletal assembly through Arp2/3 complex, implying that the WD40 repeats may have a role in interacting with actin (Welch et al., 1997). Actin-interacting protein 1 (Aip1p) is a 67-kDa protein with ten WD40 repeats and is known to regulate the depolymerization of actin filaments by cofilin (Rodal et al., 1999). Previous study has demonstrated the potential binding sites for actin which consist of WD40 repeats within Aip1p. One is the large patch of conserved residues along the circumference and bottom loops of blades 2 to 5; the other is the region between the two β -propellers within the Aip1p clamshell (Voegtli et al., 2003). Moreover, the actin-binding protein coronin-1 also known as p57 has five WD40 repeats and a coiled-coil motif. Coronin-1 forms a seven-bladed β -propeller composed of five predicted WD40 repeats and two additional blades which do not have any homology to canonical WD40 repeat (Appleton et al., 2006; Oku et al., 2003). In previous study, co-sedimentation assay is conducted to identify the precise actin-binding regions in coronin-1, and the results reveal two regions within coronin-1 are responsible for binding with actin. One is the N-terminal 34 amino acids of coronin-1 (coronin-1¹⁻³⁴), which does not contain any functional domain; the other actin binding region is coronin-1¹¹¹⁻²⁰⁴, which includes the second and third WD40 repeats (Oku et al., 2003). These results imply that WD40 repeat may be responsible for proteins to bind with actin cytoskeleton.



1.6 Membrane-bound proteins for myoblast fusion

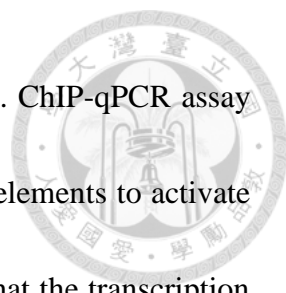
Myoblast fusion requires the fusion of membrane between two cells, so membrane-bound proteins are thought to be participate in the fusion step. Myomaker is a muscle-specific membrane protein that controls myoblast fusion and is first identified in 2013. In *in situ* hybridization, during mouse embryogenesis, myomaker gene is robustly expressed in the myotomal compartment of the somites as well as limb buds and axial skeletal muscles, which is similar to the expression pattern of *Myod* and *Myog*. Myomaker-knockout mice are found to be earlier lethality at postnatal day 7 due to muscle dysfunction. On the other hand, overexpression of myomaker in myoblasts significantly enhances fusion. Meanwhile, overexpression of myomaker in a non-fusion cell 10T1/2 fibroblasts also promotes fusion with myoblasts, demonstrating the fusogenic function of myomaker (also named as myomerger, minion) (Millay et al., 2013; Quinn et al., 2017; Zhang et al., 2017). By a genome-wide CRISPR loss-of-function screen for genes required for myoblast fusion and myogenesis, an 84-amino acid muscle-specific micropeptide--myomixer has been identified in 2017.

The expression of myomixer coincide with myoblast differentiation and is essential for myoblast fusion. Primary mouse myoblasts isolated from myomixer-knockout mice display severely impaired fusion capacity than wild-type myoblasts. Myomixer localizes to cell membrane, in which it promotes fibroblast-fibroblast fusion and



fibroblast-myoblast fusion together with myomaker, demonstrating the direct participation of these two proteins in fusion step. Thus, myomixer and myomaker are found to pair control the important step of myoblast fusion during muscle development (Bi et al., 2017). In addition, stabilin-2 is a transmembrane phosphatidylserine (PS) receptor that regulating myoblast fusion through recognition and binding with the exposed PS on myoblasts surface. Forced expression of stabilin-2 in myoblasts shows increased myotube formation, whereas deficiency of stabilin-2 results in thinner and smaller myotube. Stabilin-2-knockout mice exhibit smaller cross-sectional area (CSA) of myofibers and fewer myonuclei within each fiber than wild-type mice, indicating the reduced CSA and myonuclei number are due to the decreased myoblast fusion (Park et al., 2016). To sum up, not only actin-binding proteins but also membrane-bound proteins play important roles in myoblast fusion.

Previously, our studies discovered that the RNA and protein expression levels of myogenin are significantly lower in NRIP-gKO mice than wild-type mice at day 6 post CTX injury during muscle regeneration; also, the RNA expression level of myogenin reduces at synaptic region in cKO mice than wild-type mice (Chen et al., 2015; Chen et al., 2018), implying that the expression of myogenin may be correlated with NRIP. Moreover, myogenin has been reported to promote myoblast fusion through direct transcriptional up-regulation of *myomaker* gene (Ganassi et al., 2018). By scanning the



promoter region of *myomaker*, the authors find two E-box elements. ChIP-qPCR assay on zebrafish embryo reveals that myogenin directly binds to E-box elements to activate the transcription of myogenin. Similarly, other study also revealed that the transcription factor myogenin induce *myomaker* transcription. By analysis myomaker 5' flanking region of evolutionary conservation sequence, the authors identify two highly conserved E-boxes in close proximity to the *myomaker* transcription start site. Then they analyzed chromatin immunoprecipitation sequencing (ChIP-seq) data sets and confirm that there are significant binding of both myogenin and MyoD at these proximal E-box elements during differentiation in C2C12 muscle cell line, indicating that the myogenic transcription factor myogenin does induce myomaker expression (Millay et al., 2014). Thus, these results raising the possibility that NRIP may regulate myoblast fusion through myogenin-myomaker pathway.

1.7 Aims of the study

As mentioned above, NRIP-gKO mice display delayed skeletal muscle regeneration during muscle injury with a significant higher proportion of small-sized myofibers than wild-type mice, indicating that NRIP may regulate myoblast fusion. Myoblast fusion has been reported to be strongly associated with actin cytoskeleton remodeling and actin-binding proteins. Moreover, our unpublished studies reveal that

NRIP can interact with actin by performing *in vitro* sedimentation assay. In this study, we speculated whether NRIP could directly act through interacting with F-actin to promote myoblast fusion during myogenesis. Aims of this study are as following:

- (a) To identify the interaction of NRIP and F-actin and their subcellular localization.
 - Whether NRIP can interact with actin and which domain of NRIP is responsible for binding with actin?
 - What is the subcellular localization of NRIP in muscle cells?
- (b) To investigate whether NRIP can promote myoblast fusion.
- (c) To investigate whether NRIP promotes myoblast fusion through interacting with F-actin.
- (d) To investigate whether NRIP-induced myogenin is involved in myotube formation.

Chapter 2

Materials and methods



2.1 Generation of NRIP-knockout cell line--KO19

The CRISPR Cas9 target sites were identified at Zhang Lab's website (<http://crispr.mit.edu/>), and the pair of all-in-one plasmid constructs (L-Cas9n-EGFP and R-Cas9n-puro) were obtained from Cold Spring Biotech Corp. The two guide RNAs (gRNAs) for NRIP genome targeting were expressed by L-Cas9n-EGFP and R-Cas9n-puro, and sequences of sgRNAs were as bellow, 5'-GCC CGC ACC UGU UGU GGG AC and 5'-CUU GGG CUG GAG GAC CCG UCC. Trypsinized C2C12 cells were washed with PBS once, and 1×10^5 cells mixed with 2 μg plasmids (L-Cas9n-EGFP:R-Cas9n-puro=3:1) were used per electroporation (1650 v/ 10 ms/ 3 pulses) using Neon Transfection System 10 μl Kit (Thermo Fisher Scientific). The cells were added into 24-well plate containing antibiotic free complete medium, and incubated at 37°C overnight in a 5% CO₂ incubator. Cells were selected with 3 $\mu\text{g}/\text{ml}$ puromycin for 2 days, and then harvested. Partial of cells were analyzed the editing efficiency and the others were diluted to 0.5 cell/well and added into 96-well plate for single cell culture for one month. Half of cells in each well were purified the genomic DNA by Epicentre MasterPure DNA Purification Kit (epicentre), PCR amplified the CRISPR reaction locus with designed primer pair, and then cloned into T3 cloning kit

(ZGene Biotech) to verify the DNA sequence.




2.2 Cell culture and transfection

C2C12, KO19, 293T cells derived were cultured in DMEM with 10% fetal bovine serum, 1% penicillin-streptomycin and 1% L-glutamine. As for C2C12, KO19 differentiation, cells were washed with PBS twice and shifted to differentiation medium, which is DMEM with 2% horse serum and 1% penicillin-streptomycin, 1% L-glutamine. Cells were incubated at 37°C, 5% CO₂. 293T cells were grown to 60% confluence and transfected with target plasmids by using jetPRIME (Polyplus) as recommended by the manufacturer. For C2C12 and KO19 transfection, cells were grown to 70% confluence and transfected with target plasmids by using K2 Transfection kit (Biontexas) followed by manufacturer's instruction.

2.3 Western blots analysis

Cell lysates were harvested and extracted total protein by treating lysates with RIPA lysis buffer (150 mM NaCl, 50 mM Tris-HCl pH7.5, 10 mM EDTA, 1% NP-40) with 1% protease inhibitor and phosphatase inhibitors cocktail and incubated on ice for 25 min. Protein lysates were clarified by centrifugation at 13,200 rpm for 20 min at 4°C and the supernatant was collected and stored at -80°C. Proteins were separated on 10%



SDS-PAGE and transferred to polyvinylidene fluoride (PVDF) membranes (Millipore) for 2 hr, and then blocked in 5% BSA for 1 hr at room temperature. The membranes were then incubated with primary antibodies (Appendix), anti-NRIP (Novus, 1:2000), anti-MyHC (Abcam, 1:2000), anti-myogenin (Novus, 1:2000), anti-EGF receptor (Cell Signaling, 1:1000), anti-DsRed (TaKaRa, 1:10000), anti-GFP (Abcam, 1:10000), anti-flag (Abcam, 1:10000), anti-GAPDH (AbFrontier, 1:10000) diluted in blocking buffer and incubated overnight at 4°C. The next day, membranes were incubated with HRP-conjugated secondary antibody (1:10000) for 1 hr at room temperature. Target protein expression was detected by using an ECL western blot detection system (GE Healthcare Life Sciences).

2.4 Cytosolic and membrane protein fractionation

Cytosolic and membrane protein are extracted by using Mem-Plus Membrane Protein Extraction Kit (Thermo). Briefly, cell lysates were harvested in growth medium and centrifuged at $300 \times g$ for 5 min, and washed with Cell Wash Solution, followed by lysing the lysates with Permeabilization Buffer for 10 min with constant mixing at 4°C and centrifuged for 15 min, $300 \times g$ to obtain cytosolic fraction. Then Solubilization Buffer was added to cell pellets for 30 min with constant mixing and centrifugation at $16,000 \times g$ for 15 min to extract solubilized membrane and membrane-associated

proteins. The protein fractions of cytoplasm and membrane were analyzed by western blot.

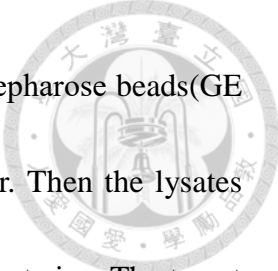


2.5 RNA extraction and RT-PCR

Cells were lysed with TRIzol Reagent (Thermo Fisher) and pipeted to homogeneity, and added 0.2 ml chloroform then incubating for 3 min at room temperature (TRIzol: chloroform=5:1). Then centrifuged the samples at $12,000 \times g$ for 15 min, and transferred the colorless upper aqueous phase containing RNA to a new tube. Adding isopropanol to the samples (RNA: isopropanol=1:1) and incubated for 10 min, followed by centrifuged at $12,000 \times g$ for 10 min, the precipitated RNA would form a white gel-like pellet at the bottom of the tube. Then washed the pellets with 75% ethanol, and centrifuged at $7,500 \times g$ for 5 min to obtain RNA. The reverse transcription was performed by using SuperScript IV Reverse Transcriptase (Invitrogen) followed by manufacturer's instruction. Then the cDNA was amplified and analyzed by PCR with indicated primers.

2.6 Immunoprecipitation assay

Equal amount of protein lysates were incubated with IP buffer (RIPA buffer without 1% NP-40, with 1% protease inhibitor and phosphatase inhibitors cocktail) and primary



antibodies at 4°C overnight with constant mixing. 50 µl Protein G Sepharose beads(GE Healthcare) were added to the lysates and incubated at 4°C for 2 hr. Then the lysates were centrifuged at 8,000 rpm, 1 min, 4°C and washed with IP buffer twice. The target protein were eluted by 3X sample dye and perform western blot subsequently.

2.7 Immunofluorescence staining

Cells were fixed with 2% PFA for 10 min and washed with PBS 3 times, followed by -20°C methanol permeated for 5 min, and blocked with 2% BSA for 30 min at room temperature. Samples were then incubated with indicated primary antibodies anti-NRIP (GeneTex, 1:200), anti-MyHC (Abcam, 1:200), anti-DsRed (TaKaRa, 1:200) and anti-GFP (Santa Cruz, 1:20) at 4°C overnight. Then samples were incubated with fluorescent secondary antibody (1:10000), phalloidin (1:1000) for 1 hr at room temperature and mounted in DAPI Fluoromount-G (SouthernBiotech). Immunostained samples were analyzed by using Carl Zeiss LSM880 confocal microscope. For quantifying myoblast differentiation and fusion, differentiation index was calculated as the percentage of nuclei in MyHC⁺ cells (including mononuclear and multinuclear cells) to the number of total nuclei. Fusion index was calculated as the percentage of nuclei contained in MyHC⁺ myotubes (at least two nuclei) to the number of total nuclei. Cells contained at least two nuclei to be considered as a myotube.



2.8 Cell fusion assay


C2C12 cells were transfected with pmCherry and KO19 transfected with pEGFP vector or pEGFP-NRIP by using K2 Transfection kit for 24 hr followed by replacing with fresh growth medium and culture for 24 hr. Then the cells were trypsinized and mixed in a ratio of 1:1 (each cell line: 0.71×10^5 cells/ cm^2) and seeded in 12-well plate covered by cover glass. The next day, cells were shifted to differentiation medium and incubated for 12 days to form fused myotubes, and then subjected to immunofluorescence staining.

2.9 Time-lapse microscopy

C2C12 myoblasts were grown to 80% confluence and cotransfected with pmCherry-actin and EGFP-NRIP by using K2 Transfection kit for 24 hr, and then shifted to differentiation medium for 48 hr. Cells were trypsinized and replated on Matrigel-coated cover glass to have proper cell density. Cells were replaced with imaging medium (phenol red-free differentiation medium) and subjected to Laser TIRF/Spinning Disc confocal Microscope for time-lapse imaging at 37°C, 5% CO_2 with time interval 10 min for 6-9 hr.

2.10 Recombinant adenovirus generation and infection

The adenovirus encoding shNRIP was constructed by inserting NRIP targeted RNAi



into pSIREN-DNR (BD Biosciences Clontech; Knockout RNAi Systems) to form pSIREN-DNR-RNAi. The pSIREN-DNR-Luc plasmid encoding an shRNA against luciferase served as a negative control. The shRNA-expressing adenovirus was generated by subcloning a functional shRNA cassette from pSIREN-DNR-RNAi into a recombinant adenovirus vector (pLP-Adeno-X-PRLS, BD Biosciences Clontech). All recombinant adenoviruses were amplified in HEK293A cells and purified by using an Adeno-XTM Maxi Purification kit (Clontech), following the manufacturer's instructions. For C2C12 knockdown assay, cells were differentiated for 3 days and infected with indicated virus with MOI=10 for 2 days, and then harvested.

2.11 Site-directed mutagenesis

Site-directed mutagenesis were performed by using Q5 Site-Directed Mutagenesis Kit (NEW ENGLAND BioLabs). pEGFP-NRIP-C Δ WD67 Δ IQ was constructed by using pEGFP-NRIP-C Δ WD67 as template to amplified the target product with indicated primers: forward 5'-GAA TTG GAT ACT TTG AAC ATT AGA CC, reverse 5'-ATC ACC AGG TCC TGC TCG AT to delete IQ motif on pEGFP-NRIP-C Δ WD67. The product was then treated with kinase, ligase and Dpn1 to ligate linear DNA into plasmid and remove template, followed by transforming into competent cells.

2.12 Statistical analysis

All statistical data were analyzed by Prism software (GraphPad Software). Data are presented as mean \pm SEM. All *P* value were determined by student's *t* test for comparison between two groups. *P* value of less than 0.05 was considered statistically significant.



Chapter 3

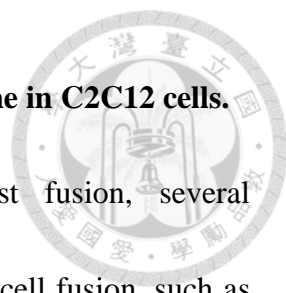
Results



3.1 NRIP reciprocally interacts with actin *in vivo*.

Previously, we demonstrated that NRIP-gKO mice display delayed skeletal muscle regeneration during cardiotoxin (CTX)-induced injury with high frequency of small myofibers compared to wild-type mice (Chen et al., 2015), suggesting that NRIP may have a role in myoblast fusion. Besides, some studies have indicated that actin-binding proteins are important for actin cytoskeleton remodeling during myoblast fusion (Berger et al., 2008; Dalkilic et al., 2006; Nowak et al., 2009; Richardson et al., 2007). Our unpublished results indicated that NRIP can interact with actin *in vitro*. Thus, we hypothesized NRIP might regulate myoblast fusion through regulating F-actin. To start this question, we first examined whether NRIP could also interact with actin *in vivo* (Won-Shin Yen's unpublished results). By performing immunoprecipitation assay in Flag-NRIP and mCherry-actin cotransfected 293T cells, we confirmed that mCherry-actin was able to be detected by immunoprecipitation of Flag tagged NRIP, and vice versa (Figure 1A-B), which further supports the preliminary studies from Won-Shin Yen on discovering the interaction of NRIP and F-actin by *in vitro* sedimentation assay. Hence, we confirmed that NRIP is a novel actin-binding protein, which can bind with actin both *in vivo* and *in vitro*.

3.2 NRIP is localized in nucleus, cytoplasm and plasma membrane in C2C12 cells.



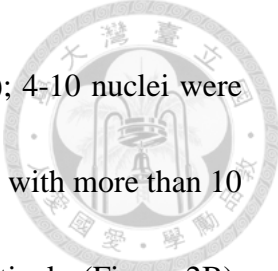
Apart from actin-binding proteins in regulating myoblast fusion, several membrane-bound proteins also have been reported to participate in cell fusion, such as myomaker, myomixer (also named myomerger and minion) and stabilin-2 (Bi et al., 2017; Millay et al., 2013; Park et al., 2016; Quinn et al., 2017; Zhang et al., 2017). Thus, we were curious about whether NRIP is a membrane-bound protein that aims for cell fusion. We examined the subcellular localization of NRIP in C2C12 by fractionate C2C12 myoblasts into cytosolic and membrane fractions. As shown in Figure 2A, NRIP was found to localize in both cytoplasm and cell membrane with nearly equal proportions (47.4% vs. 52.6%; Figure 2B), suggesting that NRIP may have its function to localize to membrane. Besides, our unpublished results from Hsin-Hsiung Chen and Yun-Hsin Huang also demonstrated NRIP was a membrane-bound protein because it could bind to acetylcholine receptor (AChR) α subunit and formed neuromuscular junction (NMJ) complex in cell membrane (Yun-Hsin Huang's unpublished results). Additionally, the immunofluorescence staining of C2C12 cells also showed that NRIP was localized to nucleus, cytoplasm and membrane (Figure 2C), which is consistent with our previous studies about NRIP functions as a transcription cofactor that expresses in nucleus (Chen et al., 2008; Tsai et al., 2005), and NRIP localized in cytoplasm to bind with CaM (Chen et al., 2015) as well as the localization of NRIP in

cell membrane to form neuromuscular junction complex (Hsin-Hsiung Chen and Yun-Hsin Huang's unpublished results).



3.3 NRIP is responsible for myotube formation.

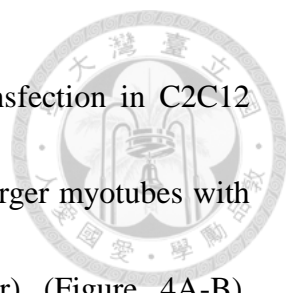
According to our studies, NRIP-gKO mice reveal significantly reduced RNA expression levels of myogenin and embryonic MyHC than wild-type mice at day 6 after CTX injury during muscle regeneration (Chen et al., 2015), indicating that NRIP may regulate myogenesis. To further investigate the role of NRIP in myogenesis, NRIP-null C2C12 cells were generated by CRISPR-Cas9 system. By targeting NRIP exon 1 by the pairs of sgRNAs resulting in frameshift mutation for NRIP deletion, NRIP-null C2C12 myoblasts were generated and named KO19 myoblasts. To examine the ability of myotube formation, C2C12 and KO19 myoblasts (Supplementary figure 1) were differentiated and immunostained with myosin heavy chain (MyHC). As shown in Figure 3A, there were extremely fewer MyHC⁺ cells in KO19 at both 5 and 8 days after differentiation than C2C12. KO19 cells hardly formed myotubes at 5 days after differentiation, while they produced a few numbers of myotubes when differentiated for 8 days. Thus, we differentiated KO19 myoblasts for 8 days in the following experiments to measure the ability of myotube formation as well as C2C12 for the consistence. KO19 formed smaller myotubes than C2C12, the percentage of myotubes containing



1-3 nuclei were 57.92% in C2C12 and 95.56% in KO19 ($P<0.0001$); 4-10 nuclei were 33.53% and 4.44% ($P<0.0001$) as well as the percentage of myotubes with more than 10 nuclei were 8.55% and 0% in C2C12 versus KO19 ($P<0.05$), respectively (Figure 2B), indicating the impaired ability of myotube formation in KO19 myoblasts. Myogenesis consists of two key steps, including myoblasts differentiating to myocytes, and myocytes fusing together to form a multinucleated myotube (Bentzinger et al., 2012; Berkes and Tapscott, 2005; Kang and Krauss, 2010; Knight and Kothary, 2011). KO19 cells showed impaired ability of myotube formation with reduced differentiation index (35.38% vs. 6.39% in C2C12 vs. KO19, $P<0.01$, Figure 3C) as well as fusion index (33.67% vs. 3.16% in C2C12 vs. KO19, $P<0.001$; Figure 3D), indicating that the inferior myotube formation may be caused by both impaired differentiation and fusion. Thus, NRIP is responsible for myoblast differentiation and myotube formation. In this study, we would focus on myotube formation.

3.4 Overexpression of NRIP in C2C12 enhances the ability of myotube formation.

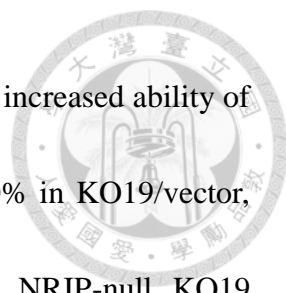
Then we confirmed the role of NRIP in myotube formation by gain of function in C2C12. C2C12 myoblasts were transfected with Flag vector or Flag-NRIP plasmids and differentiated for 8 days, then stained with anti-myosin heavy chain (MyHC) antibody (green) and DAPI for nucleus (blue) to examine myotube formation. The Flag-NRIP



expression detected by western blot confirmed the successful transfection in C2C12 (Figure 4D). Forced expression of NRIP in C2C12 contributed to larger myotubes with more nuclei, compared to control C2C12 cells (C2C12/vector) (Figure 4A-B). Consistent with the effect of NRIP displayed in C2C12 and KO19, the capacity of differentiation and fusion were both increased due to overexpression of NRIP, with the differentiation index 40.51% in C2C12/vector and 51.25% in C2C12/NRIP, $P < 0.05$; fusion index 39.48% in C2C12/vector and 50.40% in C2C12/NRIP, $P < 0.05$ (Figure 4B-C), indicating that overexpression of NRIP in C2C12 enhances the ability of myotube formation.

3.5 NRIP can rescue myotube formation in NRIP-null KO19 cells.


Similarly, KO19 myoblasts were overexpressed with NRIP to examine whether re-expression of NRIP could facilitate myoblast formation. KO19 cells were transfected with Flag vector or Flag-NRIP plasmids and differentiated for 8 days, then immunostained with myosin heavy chain (MyHC; green) to investigate the ability of myotube formation. By performing immunofluorescence assay, KO19/NRIP were discovered to have larger, longer and more myotubes than KO19/vector (Figure 5A). To quantify myoblast differentiation, we calculated the differentiation index which was significantly higher in KO19 transfected with NRIP than vector plasmids (5.72% vs.



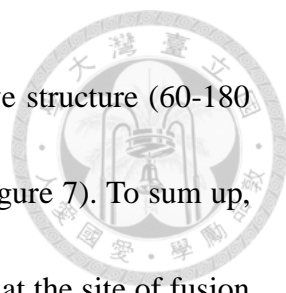
3.06%, $P < 0.05$; Figure 5B). Additionally, KO19/NRIP also revealed increased ability of myoblast fusion, with fusion index 3.37% in KO19/NRIP and 1.00% in KO19/vector, $P < 0.01$ (Figure 5C), suggesting that re-expression of NRIP in NRIP-null KO19 myoblasts can rescue myotube formation. Collectively, by loss-of-function assay, we discovered that NRIP is essential for myotube formation in comparison of C2C12 and NRIP-null KO19 myoblasts. We further confirmed the role of NRIP by overexpressing NRIP in C2C12 and KO19 myoblasts and found that both differentiation and fusion index were significantly increased in the supplement of NRIP, indicating that NRIP can enhance myotube formation through promoting myoblast differentiation and fusion in C2C12 cells; and NRIP can rescue the myotube formation in NRIP-null cells.

3.6 NRIP concentrates at the site of fusion and interacts with actin to form podosome-like structure.

Myoblast fusion can be divided into several steps, including migration, recognition, adhesion, invasion and fusion (Abmayr and Pavlath, 2012). During invasion, it is reported that asymmetrical distribution of podosome-like structure (PLS) is equipped between two fusion partners both in *Drosophila* embryo and murine myoblast C2C12 (Abmayr and Pavlath, 2012; Chuang et al., 2019). These podosome-like structures are F-actin-enriched protrusions which are important for invasion and fusion pore formation



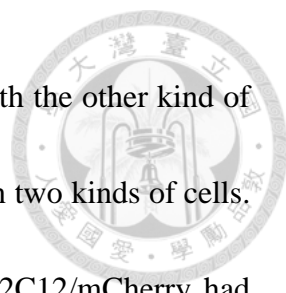
(Chen, 2011). Since we found that NRIP was an actin-binding protein (Figure 1) as well as a membrane-bound protein (Figure 2) and overexpression of NRIP can promote fusion in C2C12 and KO19 in previous studies (Figure 4-5), we speculated that whether NRIP participated in the podosome-like structure to enhance myoblast fusion. We examined C2C12 by differentiating them for 4 days and immunostained with NRIP (green) and phalloidin for F-actin (red), and discovered that NRIP concentrated at the fusion sites between myoblast and myoblast (containing one nucleus, marked by *; Figure 6A, upper panel) as well as myoblast and myotube (containing two nuclei, marked by**; Figure 6A, lower panel), suggesting that NRIP may take part in podosome-like structure to regulate myoblast fusion. During cell fusion, the asymmetrical distribution of podosome-like structure is located at the attacking cell in one of the two myoblasts (Abmayr and Pavlath, 2012; Chuang et al., 2019). To examine whether NRIP involved in podosome-like structure, we performed time-lapse microscopy to observe the dynamics of NRIP and actin in C2C12 during myoblast fusion. C2C12 cells were cotransfected with EGFP-NRIP and mCherry-actin by K2 Transfection kit for 24hr and shifted to differentiation medium for 24hr, then trypsinized and replated on Matrigel-coated cover glass and subjected to time-lapse microscopy. We observed that EGFP-NRIP and mCherry-actin colocalized and concentrated to form actin and NRIP-enriched foci in cytoplasm of C2C12 (0-30min), and then the foci



protruded toward cell membrane to form a podosome-like protrusive structure (60-180 min) which might participate in invasion during myoblast fusion (Figure 7). To sum up, we observed the asymmetrical distribution of F-actin enriched focus at the site of fusion. Meanwhile NRIP also formed a focus and colocalized with F-actin to exhibit a podosome-like structure and elongated over the time course, which further supports our hypothesis that NRIP interacts with actin to promote myoblast fusion.

3.7 NRIP promotes myoblast fusion.

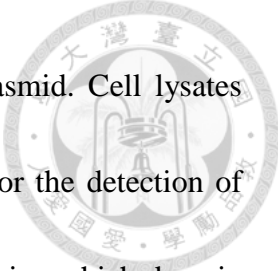
Apart from the observation of NRIP and actin-enriched podosome-like structure at the fusion site, NRIP-gKO mice has been reported to displayed higher proportion of small-sized myofibers during muscle regeneration (Chen et al., 2015), which suggesting that NRIP may regulate myoblast fusion. To answer this question, we performed cell fusion assay to figure out whether NRIP can promote myoblast fusion. C2C12 cells were transfected with mCherry vector to have red color; KO19 (NRIP-null) cells were transfected with EGFP vector as control group or EGFP-NRIP as experimental group, and displayed green color, respectively. Then, C2C12 and KO19 were mixed together in a ratio of 1 to 1 (each cell line: 0.71×10^5 cells/ cm^2), and shifted to differentiation medium for 12 days to form myotubes (Figure 8A). The mixed cells were stained with anti-EGFP and anti-DsRed for mCherry to enhance the fluorescence intensity. Only



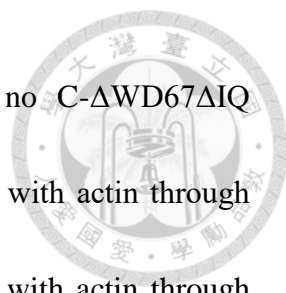
EGFP⁺ (green) or mCherry⁺ (red) cells indicate they did not fuse with the other kind of cells, while co-positive cells represented the fusion occurred between two kinds of cells. Both KO19/EGFP + C2C12/mCherry and KO19/EGFP-NRIP + C2C12/mCherry had co-positive myotubes, while KO19/EGFP-NRIP showed larger fused myotubes with more myonuclei (marked by arrow; Figure 8B). The quantitative data was calculated as the number of co-positive myotubes with at least three nuclei to total number of co-positive myotubes; the result revealed that KO19/EGFP-NRIP + C2C12/mCherry displayed larger co-positive myotubes with at least 3 myonuclei compared to control group KO19/EGFP + C2C12/mCherry (KO19/EGFP + C2C12/mCherry set as 1; 1.23 vs. 1, $P < 0.05$; Figure 8C), indicating that fusion capacity was improved with the supplement of NRIP. Collectively, both high concentration of NRIP at cell-cell contact sites and the increased proportion of fused myotube with more nuclei suggest that NRIP positively regulates myoblast fusion.

3.8 NRIP may directly interact with actin through WD67 domains and indirectly bind with actin through IQ motif in an ACTN2-dependent manner.

As shown in Figure 1, we have confirmed that NRIP could interact with actin *in vivo*. Next, we further investigated which domain of NRIP is responsible for binding with actin. To perform immunoprecipitation assay, 293T cells were transiently



co-transfected with NRIP truncated mutants and mCherry-actin plasmid. Cell lysates were extracted and immunoprecipitated with anti-DsRed antibody for the detection of mCherry-actin. Different NRIP truncated mutants were used to examine which domain could interact with actin, including NRIP-FL (containing WD1-7 domains and one IQ motif), NRIP- Δ IQ (containing WD1-7 domains without IQ motif), NRIP-C (containing WD67 domains and one IQ motif), C- Δ WD67 (containing one IQ motif), C- Δ WD67 Δ IQ (C-terminus without WD67 domains, IQ domain) and WD67 (containing WD67 domains; Figure 9A). The results revealed that four NRIP mutants, including NRIP-FL, NRIP- Δ IQ, NRIP-C and C- Δ WD67 were able to bind with actin (Figure 9B). Among them, NRIP- Δ IQ which only contains seven WD40 domains could interact with actin, suggesting that WD40 domain may be the domain to bind with actin. Besides, C- Δ WD67 with only one IQ motif also could bind with actin. NRIP has been reported to interact with EF-hand of ACTN2 through its IQ motif in our previous studies (Szu-Wei Chang and Ssu-Yu Lin's unpublished results), and ACTN2 is known as an actin-binding protein (Mimura and Asano, 1986). Thus, the interaction between C- Δ WD67 and actin may be through its IQ motif to indirectly bind with actin in an ACTN2-dependent manner. In order to confirm our hypothesis, we constructed C- Δ WD67 Δ IQ plasmid (Supplementary figure 3) to verify that IQ domain of NRIP also contributes to binding with actin. By performing immunoprecipitation assay with

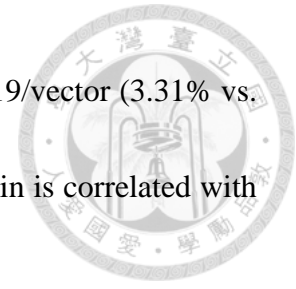


C- Δ WD67 Δ IQ and actin, as shown in Figure 9C, there was no C- Δ WD67 Δ IQ precipitated by actin, confirming that C- Δ WD67 indirectly interact with actin through ACTN2. Moreover, previous study illustrated that coronin-1 binds with actin through coronin-1¹¹¹⁻²⁰⁴, which includes two WD40 domains (Oku et al., 2003), indicating that WD40 domains may bind with actin. Thus, we performed immunoprecipitation assay to check whether NRIP binds with actin through WD40 domains. The result revealed that WD67 could be detected when immunoprecipitated with actin, confirming that WD67 domains are responsible for NRIP to bind with actin (Figure 9D). The result is similar with coronin-1 binding with actin through WD40 domains (Oku et al., 2003).

3.9 The WD67 domains of NRIP are related to myotube formation.

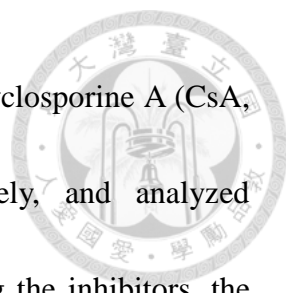
Actin cytoskeleton remodeled by actin-binding proteins play an important role in myoblast fusion. Here we have identified that the WD67 domains of NRIP are responsible for binding with actin, so we were curious about whether NRIP binding with actin is related to myoblast fusion. KO19 myoblasts were transfected with WD67 plasmid which can bind with actin (Figure 9D) and shifted to differentiation medium for 8 days, then stained myosin heavy chain (MyHC; green) and DAPI for nucleus (blue) to examine myotube formation. The differentiation index significantly increased in KO19/WD67 than KO19/vector (7.02% vs. 4.74%, $P < 0.01$; Figure 10B). Fusion index

was significantly enhanced in KO19/WD67 group compared to KO19/vector (3.31% vs. 2.00%, $P < 0.05$; Figure 10B), suggesting that NRIP binding with actin is correlated with myotube formation.



3.10 Knockdown of NRIP down-regulates the RNA and protein expression levels of myogenin and MyHC during C2C12 differentiation.

Previously, our study discovered that the RNA and protein expression levels of myogenin are significantly lower in NRIP-gKO mice than wild-type mice at day 6 post CTX injury during muscle regeneration (Chen et al., 2015). Also, our recent study demonstrates that the RNA expression level of myogenin reduces at synaptic region in cKO mice than wild-type mice (Chen et al., 2018), indicating that the expression of myogenin may be correlated with NRIP. Moreover, our studies indicate that in the presence of Ca^{2+} , NRIP can bind with CaM through its IQ motif to activate downstream phosphatase CaN and calmodulin kinase II (CaMKII) (Chen et al., 2015), which have been reported to promote myogenin expression (Friday et al., 2003; Tang et al., 2004). Thus, we used corresponding inhibitors of CaM, CaN, and CaMKII to investigate the NRIP regulated myogenin pathway. By using RT-qPCR analysis, the RNA expression level of myogenin in C2C12 infected with Ad-NRIP increased about two fold (Supplementary figure 2B-D, lane 2). In addition to infecting C2C12 with Ad-NRIP, we



also co-treated cells with relative inhibitors, W7 (CaM inhibitor), cyclosporine A (CsA, calcineurin inhibitor) or KN93 (CaMKII inhibitor), respectively, and analyzed myogenin RNA level. The results showed that upon administrating the inhibitors, the Ad-NRIP-induced up-regulation of myogenin was diminished (Supplementary figure 2B-D, lane 4), which confirms our hypothesis about that NRIP activates myogenin expression through CaM to activate CaN and CaMKII signaling. Moreover, myogenin has been reported to promote myoblast fusion through direct transcriptional up-regulation of *myomaker* gene (Ganassi et al., 2018). Thus, we hypothesized that NRIP may also regulate myotube formation through myogenin. To confirm the hypothesis, we first examined whether the RNA expression level of myogenin was down-regulated when NRIP was knockdown during C2C12 differentiation. C2C12 cells were differentiated for 3 days, and NRIP was knockdown by infecting adenovirus encoding shNRIP (named Ad-shNRIP, MOI=10; (Chen et al., 2018) or shLuc (named Ad-shLuc, MOI=10) as control for 2 days. The result showed that RNA expression level of myogenin was significantly reduced in Ad-shNRIP infected C2C12 than Ad-shLuc group (shLuc set as 1; shNRIP 0.48, $P<0.01$; Figure 12A-B). Moreover, the protein expression levels of myogenin and MyHC were also decreased in shNRIP group than shLuc group (shLuc set as 1; shNRIP 0.71, $P<0.05$; shNRIP 0.66, $P<0.05$, respectively; Figure 12C-E), showing that knockdown of NRIP results in the reduction of myogenin

and MyHC, which indicates the impaired ability of myotube formation.



Chapter 4

Discussion




In this study, we focus on the role of NRIP through binding with actin to regulate myoblast fusion. First, we confirmed that NRIP can bind with actin *in vivo*, which further support our previous finding about NRIP interact with F-actin *in vitro*. In this study, we performed immunoprecipitation assay by cotransfecting NRIP and actin to 293T cells, and verified the reciprocal interaction between NRIP and actin *in vivo* (Figure 1). Actin is the most abundant protein in eukaryotic cells, and plays critical role in many cellular functions, including cell motility, maintenance of cell shape and polarity and regulation of transcription (Dominguez and Holmes, 2011). Thus, being an actin-binding protein, it is interesting to further investigate the role of actin bound NRIP.

Apart from NRIP is an actin-binding protein, we also discovered that NRIP is a membrane-bound protein. Consistently, our previous studies have reported that by performing immunoprecipitation assay, NRIP is found to interact with AChR α subunit which is a membrane-bound receptor, and NRIP also colocalizes with AChR, rapsyn and ACTN2 to form neuromuscular junction complex (NMJ; Hsin-Hsiung Chen and Yun-Hsin Huang's unpublished results), suggesting that NRIP may localize in membrane. We further performed cytosolic and membrane protein fractionation and found that there were approximately 50% of NRIP presented in the membrane fraction,

confirming NRIP as a membrane-bound protein; and further confirmed by IFA (Figure 2). Collectively, NRIP is a novel actin-binding protein and membrane-bound protein.

Not only actin-binding proteins but also membrane-bound proteins have been reported to positively regulate myoblast fusion (Berger et al., 2008; Millay et al., 2013; Park et al., 2016). Our previous studies also demonstrate that NRIP-gKO mice exhibited higher proportion of small-sized myofiber during muscle regeneration (Chen et al., 2015), indicating that NRIP may have a role in myoblast fusion. In this study, we demonstrate that NRIP is responsible for myotube formation. We examined the ability of myotube formation in C2C12 and NRIP-null KO19 myoblasts generated by CRISPR-Cas9 system. Both differentiation and fusion capacity were dramatically reduced in KO19 cells compared to C2C12. In addition, overexpression of NRIP in C2C12 can enhance myotube formation; and NRIP in NRIP-null KO19 could rescue the ability of myotube formation (Figure 3-5). These results suggest that NRIP can enhance myotube formation through fusion. Furthermore, we also discovered that NRIP promotes myoblast fusion directly by cell fusion assay which is frequently used to investigate the fusogenic activity of a protein (Millay et al., 2013; Park et al., 2016). We found that the proportion of fused myotube with at least three nuclei is higher in KO19/EGFP-NRIP + C2C12/mCherry than KO19/EGFP + C2C12/mCherry, indicating that fusion capacity is promoted in the presence of NRIP (Figure 8). Stabilin-2 is a




phosphatidylserine (PS) receptor located in cell membrane and is reported to enhance the efficiency of myoblast fusion during myogenic differentiation and muscle regeneration (Park et al., 2016). Stabilin-2-deficient myoblasts display significantly reduced fusion index with fewer myonuclei in myotubes, which resembles NRIP-knockout KO19 myoblasts. Moreover, stabilin-2-knockout mice exhibit fewer large myotubes and decreased number of centralized nuclei, suggesting that impaired regeneration in stabilin-2-knockout mice is due to defective myoblast fusion. However, the fusion phenotype is relatively mild in stabilin-2-deficient mice which are not embryonic lethal, and are similar with NRIP-cKO mice. Thus, the author considers stabilin-2 is not essential for myoblast fusion *in vivo* but is important to modulate the fusion efficiency. Since NRIP-cKO mice are not lethal, there may be other proteins to compensate its function *in vivo*, or NRIP is like stabilin-2 just to promote the efficiency of myoblast fusion.

Alike NRIP, there are several actin-binding proteins involved in cell fusion. For example, FilaminC is also an actin-binding protein and found to control myogenesis by regulating differentiation and fusion. Knockdown of FilaminC in C2C12 shows decreased protein expression level of myogenin as well as lower RNA expression levels of muscle-specific genes caveolin3, myotilin, and $\alpha 7$ integrin, which is similar with our finding that NRIP-gKO mice displayed reduced RNA level of myogenin during muscle

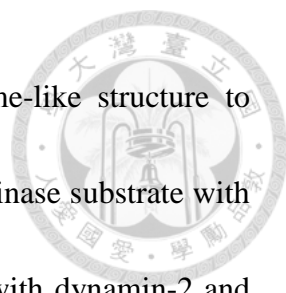
regeneration (Chen et al., 2015). Moreover, FilaminC-knockdown C2C12 cells fail to form elongated myotubes but form multinucleated “myoballs” and fuse at a slower rate.

There are several kinds of actin-binding proteins, including actin-nucleation, cross-linking, capping protein and so on. Among them, FilaminC is an actin-cross-linking protein and according to Won-Shin Yen’s unpublished research, NRIP facilitates ACTN2-dependent bundling of actin filaments in *in vitro* low-speed F-actin bundling assay, raising the possibility that NRIP may serve as an actin-cross-linking protein, too. In addition, FilaminC-deficient mice are neonatally lethal, while NRIP-cKO mice are not. Thus, it may be interesting to further investigate the mechanism of actin-binding protein regulated myotube formation. In addition, Arp2/3 complex and SCAR/WAVE are both actin-nucleation proteins function in promote actin polymerization. Arp2/3 complex promotes the formation of new actin filaments by binding to pre-existing actin filaments and branching. SCAR/WAVE pentameric complex promotes actin polymerization by activating Arp2/3 complex (Berger et al., 2008). Either *SCAR* or *Arp3* loss-of-function mutants in *Drosophila* exhibit impaired capacity of myoblast fusion with enlarged actin foci accumulated at cell contact site (Berger et al., 2008; Richardson et al., 2007), which shows the impaired actin reorganization ability. Thus, the results indicate that by remodeling actin cytoskeleton at the site of cell-cell contact, these actin-binding proteins are essential in

promoting myoblast fusion.

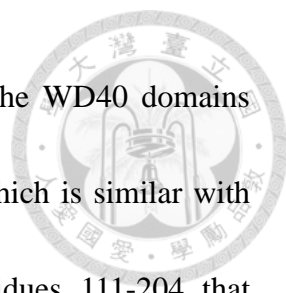


NRIP concentrates at fusion site to form podosome-like structure. During myoblast fusion, the asymmetrical distribution of the F-actin-enriched podosome-like structure (PLS) is important for invasion and fusion pore formation (Sens et al., 2010). In *Drosophila*, due to different behaviors during fusion, the two fused partners are divided into two types of cells: founder cells and fusion competent myoblasts (FCMs), which are specified by the action of transcription factors (Chen and Olson, 2004; Kim et al., 2015). Muscle founder cells act as “attractants” for surrounding FCMs to fuse with them. During fusion, FCMs generate F-actin-enriched invasive podosome-like structure to invade into founder cells and result in fusion pore formation. As for founder cells, they exhibit a thin sheath of F-actin along the founder cell membrane at the fusogenic synapse (Kim et al., 2015; Sens et al., 2010). In this study, we found that NRIP concentrates at fusion site and interacts with actin to form podosome-like structure, which may promote myoblast fusion. In the immunofluorescence staining of C2C12, we observed NRIP asymmetrically concentrated at myoblast-myoblast and myoblast-myotube contact sites (Figure 6). Furthermore, by time-lapse imaging, it revealed that actin and NRIP colocalized and concentrated to form actin-NRIP foci in cytoplasm of C2C12, and then protruded toward cell membrane forming a podosome-like structure during myoblast fusion (Figure 7). By binding with actin, NRIP



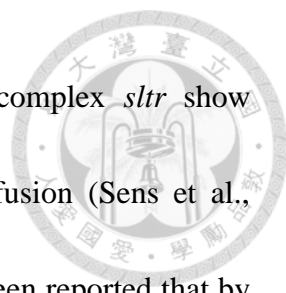
seems to enhance the structural integrity of actin-based podosome-like structure to promote invasion during fusion. Recent studies show that tyrosine kinase substrate with 5 SH3 domain (Tks5), as a component of podosome, can interact with dynamin-2 and modulate its assembly into helices around actin filaments to enhance actin bundle rigidity in invadosomes to promote myoblast fusion (Chuang et al., 2019; Thompson et al., 2008). By using atomic force microscopy (AFM) to measure topography and stiffness, it is found that in the presence of Tks5, the stiffness of dynamin-2-actin bundles increases in invadosome, and thus promote invasion during myoblast fusion (Chuang et al., 2019). Notably, in our studies, we also learned that NRIP concentrates and colocalizes with actin to form a NRIP- and F-actin-enriched foci, which may participate in invasion during fusion. Both Tks5, dynamin-2 and NRIP are found to concentrate at the tips of differentiated myoblasts, suggesting that NRIP may be involved in one of the components of invadosome. Thus, it will be interesting to investigate whether the NRIP-promoted myoblast fusion is correlated with invadosome.

Upon realizing NRIP is an actin-binding protein, we further dissected which domain of NRIP is responsible for binding with actin, and demonstrated that NRIP directly binds with actin through WD67 domains and indirectly interacts with actin through IQ motif in an ACTN2-dependent manner. Our immunoprecipitation assay reveals that both NRIP- Δ IQ (containing WD1-7 domains without IQ motif) and WD67

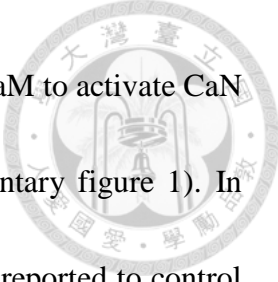


(containing WD67 domains) can bind with actin, indicating that the WD40 domains especially WD67 of NRIP is essential for interaction with actin, which is similar with previous study about that coronin-1 binds to actin through residues 111-204 that includes two WD40 domains (Oku et al., 2003). Moreover, we also discovered the interaction between C- Δ WD67 (containing one IQ motif) and actin, suggesting that there may be an indirect binding of NRIP and actin through ACTN2. We further confirmed our hypothesis by performing immunoprecipitation assay with C- Δ WD67 Δ IQ (C-terminus without WD67 domains, IQ domain) and actin, and found that there was no interaction between C- Δ WD67 Δ IQ and actin, which verified that the IQ motif also contributes to the interaction between NRIP and actin indirectly through ACTN2 (Figure 9). These results are also consistent with previous studies about that NRIP can interact with EF-hand of ACTN2 through its IQ motif (Szu-Wei Chang and Ssu-Yu Lin's unpublished results), and ACTN2 is known as an actin-binding protein (Mimura and Asano, 1986).

Actin cytoskeleton remodeled by actin-binding proteins is an essential process during myoblast fusion, such as the reorganization of actin to form podosome-like structures, lamellipodia and filopodia (Nowak et al., 2009; Sens et al., 2010). Previous studies indicate that WASP and Scar complexes are required for F-actin foci formation. Both WASP and SCAR complexes activate Arp2/3 complex to promote actin



polymerization. Mutations in *scar* and a component of WASP complex *sltr* show dramatic reduction in F-actin size, and severely block myoblast fusion (Sens et al., 2010). In addition, dynamin-2 is an actin-binding protein, and has been reported that by interacting with Tks5, dynamin-2 assembles better into helixes around actin filaments to increase the rigidity of actin bundle in invadosome, and thus promote myoblast fusion (Chuang et al., 2019). These all suggest that actin-binding proteins are essential for myoblast fusion through regulating actin cytoskeleton. In this study, we demonstrated that NRIP binding with actin may be correlated with myoblast fusion. By transfecting KO19 with WD67 plasmid which is responsible for binding with actin and then examining myotube formation, it showed that the fusion capacity was significantly higher in KO19/WD67 group than KO19/vector (Figure 10), implying the relationship between NRIP binding with actin and myoblast fusion. By binding with actin, NRIP may act to enhance the structural integrity of podosome-like structure to promote invasion during myoblast fusion, which is similar with Tks5 and dynamin-2-mediated invadosome (Chuang et al., 2019). Because the differentiation capacity in KO19 are severely impaired and may not be suitable to examine myotube formation, thus, C2C12 which differentiate normally will be a better model to investigate whether NRIP binding with actin is correlated to myoblast fusion. In the future, we will use C2C12 transfected with different NRIP truncated mutants to verify our hypothesis.



NRIP can activate myogenin expression through binding with CaM to activate CaN and CaMKII signaling to promote myogenin expression (supplementary figure 1). In addition to actin-regulated myoblast fusion, myogenin has also been reported to control fusion (Ganassi et al., 2018). Here, we further demonstrated that knockdown of NRIP down-regulates myogenin and MyHC during C2C12 differentiation to verify that NRIP-induced myogenin through binding with CaM to activate CaN and CaMKII signaling (supplementary figure 1). In this study, we performed Ad-shNRIP to knockdown NRIP, and the results showed that the RNA and protein expression level of myogenin as well as MyHC decreased, which indicates that the ability of myotube formation is impaired and may downregulate myoblast fusion because myogenin can regulate *myomaker* transcription. Thus, we can examine myomaker expression in NRIP-knockdown C2C12 to further support that NRIP regulates myoblast fusion through myogenin-myomaker pathway. As shown in Figure 3 and 4, NRIP could affect differentiation, but we did not further characterize it. Based on our previous study, the RNA expression of desmin which is a marker of differentiation decreases in NRIP-gKO mice during muscle regeneration (Chen et al., 2015), suggesting that NRIP may play a role in differentiation. In the future, we will further characterize the role of NRIP in differentiation.

In summary, NRIP acts as an actin-binding protein to promote myoblast fusion and

also upregulates myogenin expression through binding with CaM to activate CaN and CaMKII signaling pathway that may be the other reason to promoter myotube formation.

Collectively, these findings help us to get a deeper understating about the molecular mechanism during myoblast fusion, and NRIP enhanced muscle cell fusion may be a strategy for better muscle repair.

Chapter 5

Figures

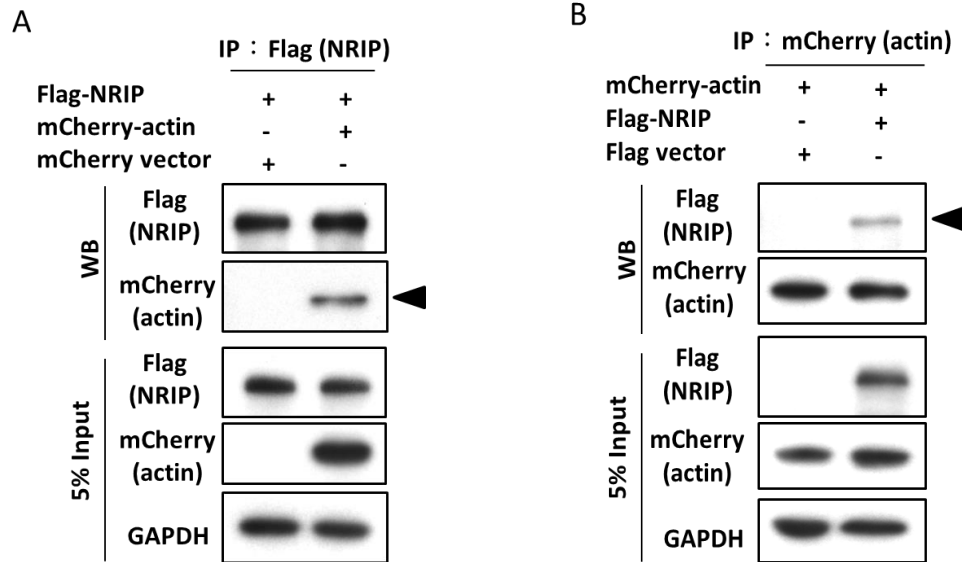


Figure 1. NRIP reciprocally interacts with actin in cells.

(A, B) Immunoprecipitation assay of NRIP and actin. 293T cells were transiently cotransfected by jetPRIME with (A) Flag-NRIP and either mCherry-actin or mCherry vector plasmid. (B) Reciprocally, mCherry-actin and either Flag-NRIP or Flag vector plasmid. Cell lysates were extracted and incubated with (A) anti-Flag (B) anti-DsRed (for mCherry) antibodies to perform immunoprecipitation assay and western blot. mCherry and Flag vector were used as negative controls. Arrowheads indicate the target protein. NRIP can reciprocally interact with actin *in vivo*.

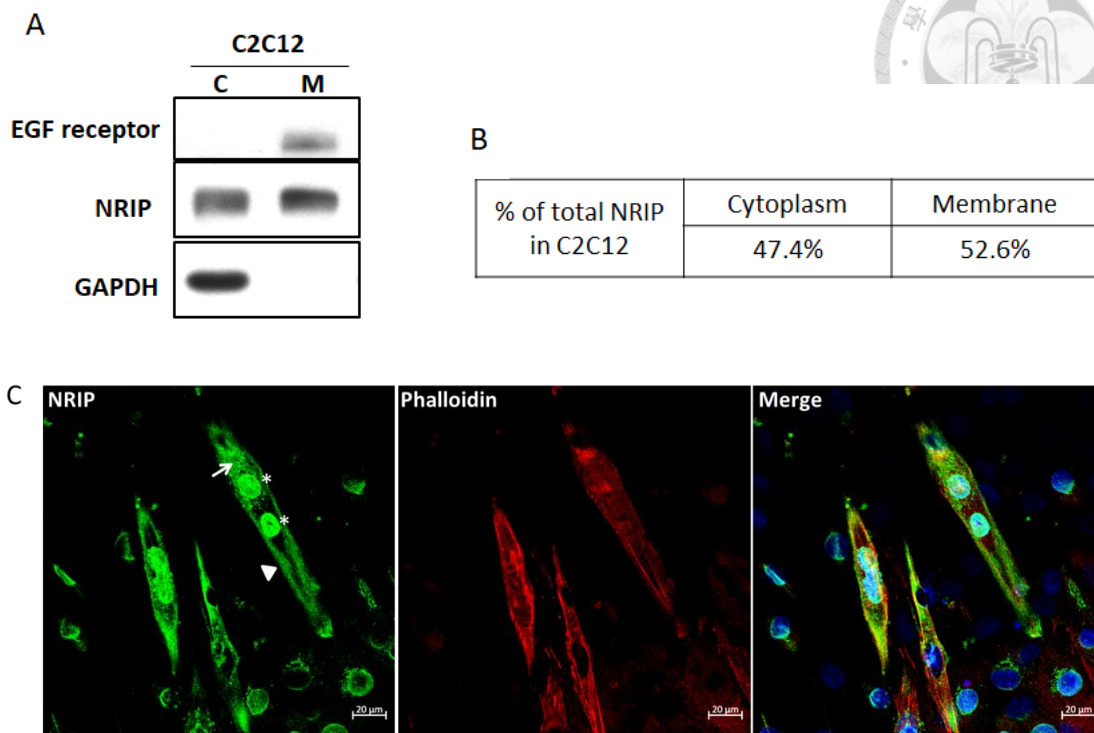


Figure 2. NRIP is a membrane-bound protein in C2C12 cells.

(A) C2C12 cell (undifferentiated) were harvested and extracted cytosolic protein by incubating cell lysate in Permeabilization Buffer (from Mem-PER Plus) for 10 min and centrifuge for 15 min, $300 \times g$ to obtain cytosolic fraction, followed by adding Solubilization Buffer to cell pellets for 30 min and centrifugation at $16000 \times g$ for 15 min to extract solubilized membrane and membrane-associated proteins. Cytosolic (C) and membrane (M) fractions of C2C12 cells are detected by western blot. Epidermal growth factor (EGF) receptor was used as a positive control of membrane protein. GAPDH was used as a positive control of cytosolic proteins. The localization of NRIP could be found both in cytoplasm and membrane in C2C12 cells. (B) Statistical results. The percentage of cytosolic and membrane-bound NRIP is 47.4% versus 52.6%. The ratio was counted by cytosolic or membrane NRIP/ cytosolic + membrane NRIP (total NRIP) and measured by ImageJ software. (C) C2C12 cells were differentiated for 4 days, and fixed with 4% paraformaldehyde, followed by immunofluorescence staining of NRIP (green), phalloidin for cell membrane (red, F-actin staining), and DAPI for nucleus (blue). NRIP was localized in nucleus (asterisk), cytoplasm (arrow) and cell membrane (arrowhead). Scale bar: $20\mu\text{m}$.

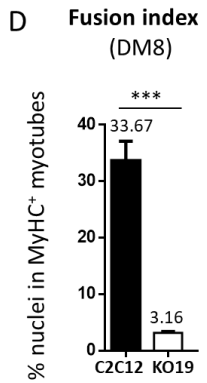
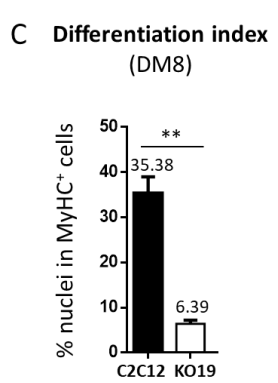
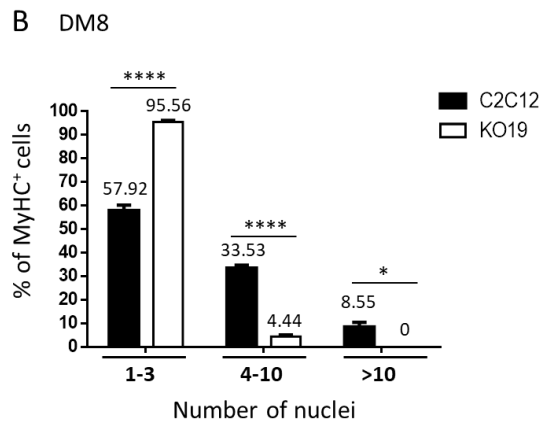
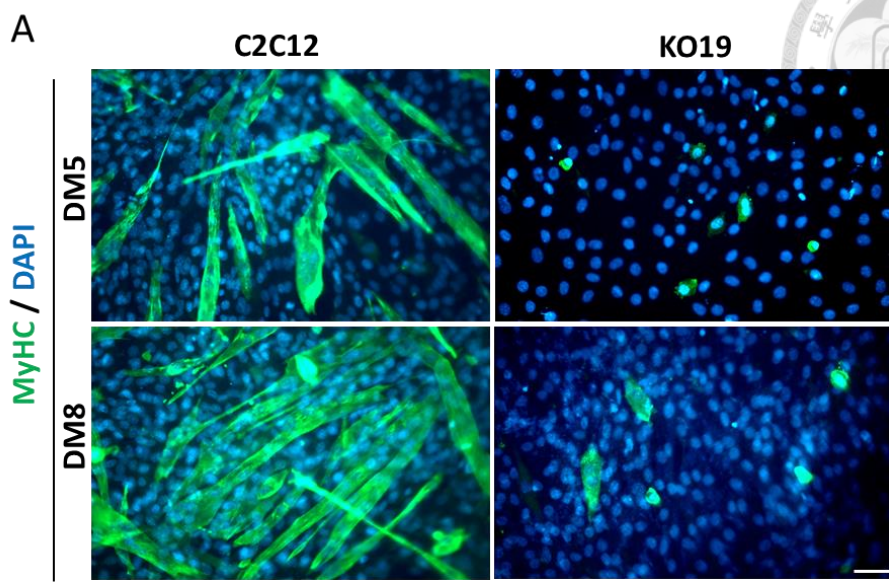
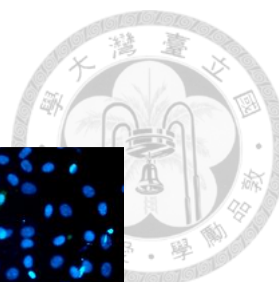


Figure 3. Generation of NRIP-null C2C12 cells which lose the ability of myotube formation.

NRIP-null C2C12 cells were generated by CRISPR-Cas9 system. NRIP gene consists of 19 exons with the translation start site at exon 1. By targeting NRIP exon 1 by the pairs of sgRNAs resulting in frameshift mutation for NRIP deletion, NRIP-null C2C12

myoblasts were generated and named KO19 myoblasts. (A) C2C12 and KO19 cells were differentiated for 5 or 8 days separately, and stained with anti-myosin heavy chain (MyHC) antibody (green) and DAPI for nucleus (blue). KO19 cells hardly form myotubes at 5 days after differentiation (DM5), while they produced a few numbers of myotubes when differentiated for 8 days (DM8). Thus, we differentiate KO19 myoblasts for 8 days in the following experiments to measure the ability of myotube formation. As shown in (A), there were extremely fewer MyHC⁺ cells in KO19 at both 5 and 8 days after differentiation than C2C12. Scale bar: 100 μ m. (B) The percentage of myonuclei number distribution at differentiation 8 days of C2C12 and KO19. Categorizing myonuclei number in three groups: 1-3 nuclei, 4-10 nuclei and >10 nuclei. KO19 cells displayed a higher proportion of less-nuclei myotubes than C2C12 cells (DM8; 1-3 nuclei 57.92 vs. 95.56%, $P<0.0001$; 4-10 nuclei 33.53% vs. 4.44%, $P<0.0001$; >10 nuclei 8.55% vs. 0%, $P<0.05$ in C2C12 vs. KO19, respectively) (C) Differentiation index indicates the ability of myoblasts differentiating to myocytes, which calculated as the percentage of nuclei in MyHC⁺ cells (including mononuclear and multinuclear cells) to the number of total nuclei. C2C12 displayed better differentiation ability than KO19 (35.38% vs. 6.39%, $P<0.01$) (D) Fusion index indicates the capacity of mononuclear myocytes fusing together to form a multinucleated myotube, which calculated as the percentage of nuclei contained in MyHC⁺ myotubes (at least two nuclei) to the number of total nuclei. The fusion index was approximately ten-fold lower in KO19 than C2C12 (DM8; 3.26% vs. 33.67%, $P<0.001$). N=3, data are presented as mean \pm SEM. ** $p<0.01$ and *** $p<0.001$; Student's t-test.

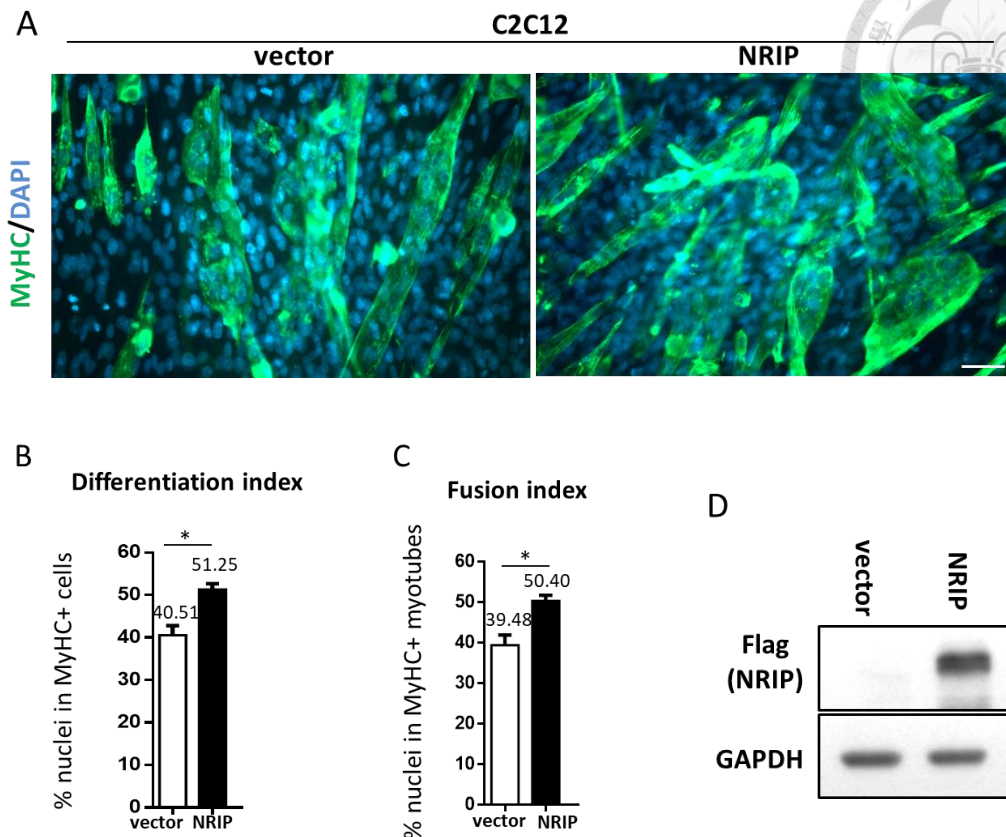


Figure 4. Overexpression of NRIP in C2C12 enhances the ability of myotube formation.

(A) C2C12 cells were transfected with Flag vector or Flag-NRIP plasmid for 24hr and shifted to differentiation medium for further 8 days incubation, then stained with anti-myosin heavy chain (MyHC) antibody (green) and DAPI for nucleus (blue) to examine myotube formation, scale bar: 100 μ m. (B) Differentiation index and (C) fusion index were calculated as shown in Figure 3 (C, D). (B) Differentiation index was higher in C2C12 transfected with NRIP than vector (51.25% vs. 40.51%, $P < 0.05$). (C) Quantitative data revealed that the fusion index in C2C12 transfected with NRIP was higher than vector group (50.40% vs. 39.48%, $P < 0.05$). $N = 3$, data are presented as mean \pm SEM. * $p < 0.05$; Student's t-test. (E) The protein expression of Flag-NRIP in C2C12 cells transfected by K2 Transfection kit and detected by western blot.

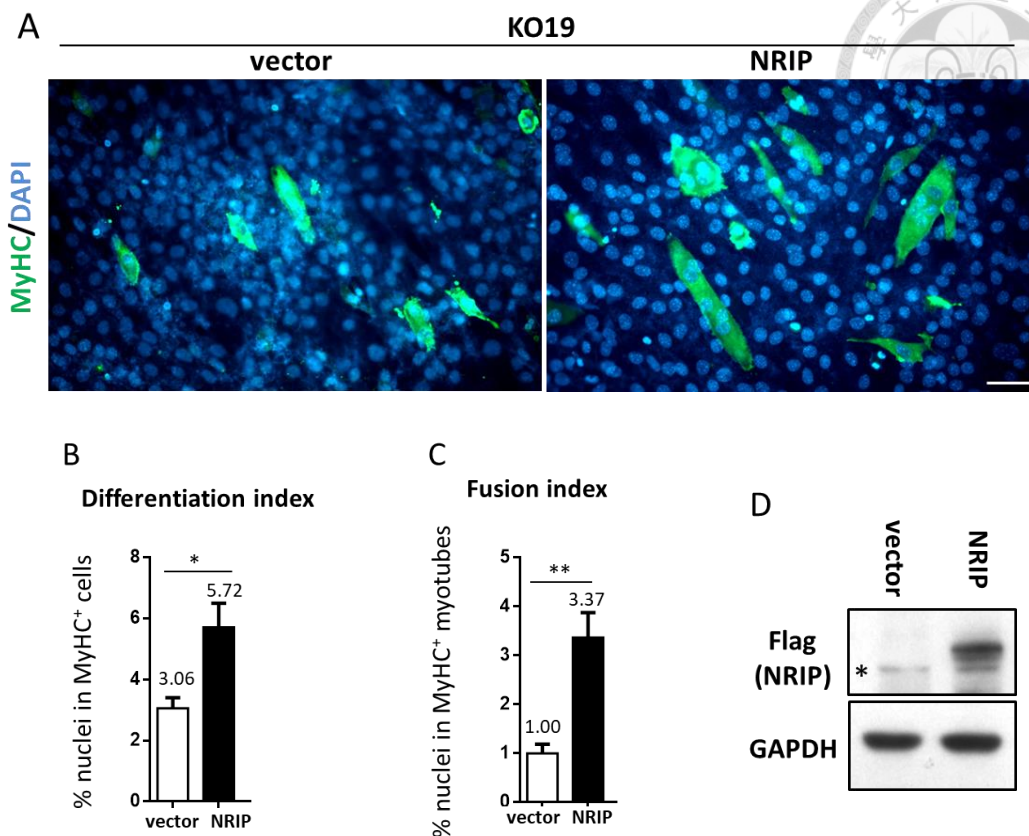


Figure 5. NRIP can rescue myotube formation in NRIP-null KO19 cells.

(A) KO19 cells were transfected with Flag vector or Flag-NRIP plasmid for 24 hr and shifted to differentiation medium for 8 days, then stained with anti-myosin heavy chain (MyHC) antibody (green) and DAPI for nucleus (blue) to examine myotube formation, scale bar: 100 μ m. (B) Differentiation index and (C) fusion index were calculated as shown in Figure 3 (C, D). (C) Quantitative result revealed that the differentiation index was about 1.8-fold higher in KO19/NRIP than KO19/vector (5.72% vs. 3.06%, $P < 0.05$). (D) Fusion index increased about 3-fold in KO19/NRIP compared to KO19/vector (3.37% vs. 1.00%, $P < 0.01$), indicating that the ability of myotube formation was significantly restored in NRIP-overexpressed KO19 cells. $N = 5$, data are presented as mean \pm SEM. * $p < 0.05$ and ** $p < 0.01$; Student's t-test. (D) The protein expression of Flag-NRIP in KO19 cells transfected by K2 Transfection kit and detected by western blot. Asterisk indicates non-specific band.

A

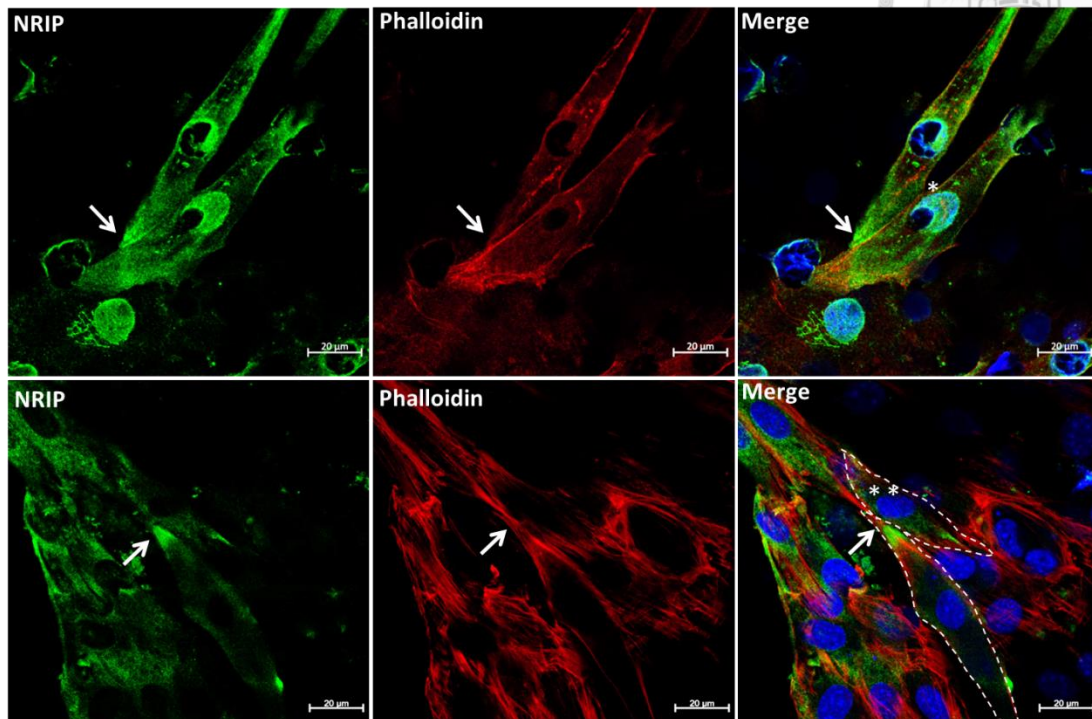


Figure 6. NRIP concentrates at the contact sites between myoblast and myoblast (or myotube).

C2C12 were differentiated in differentiation medium for 4 days, then fixed the cells with 4% paraformaldehyde, followed by immunostained with NRIP (green), phalloidin for cell membrane (red, F-actin staining), and DAPI for nucleus (blue), asterisk indicates nucleus, and white arrows indicate the concentrated site of NRIP at cell-cell contact area. NRIP locates at the contact sites between myoblast and myoblast (upper panel) as well as myoblast and myotube (lower panel), indicating that NRIP may involve in myoblast or myotube fusion. Scale bar: 20μm.

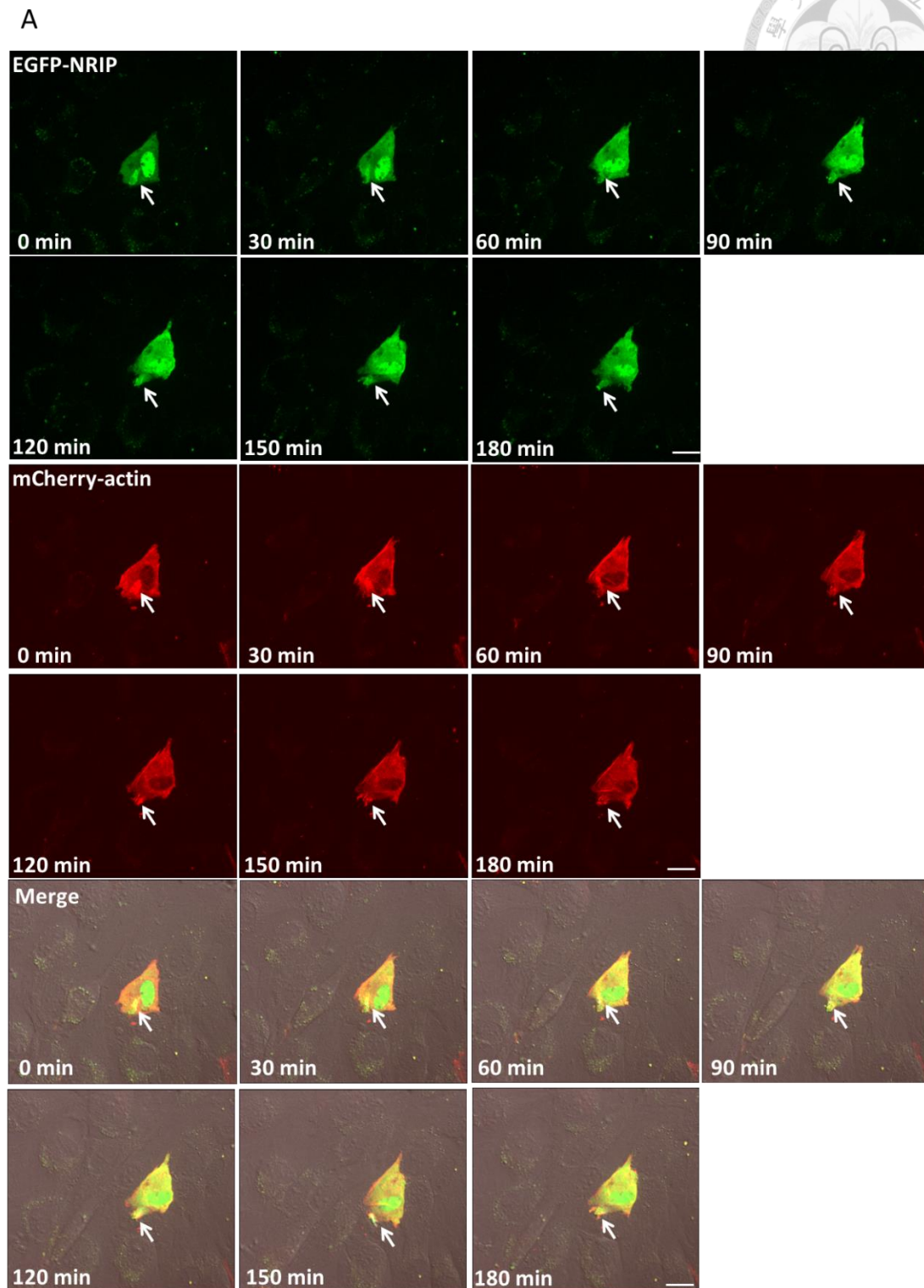
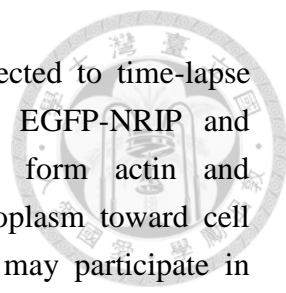


Figure 7. NRIP interacts with F-actin to form podosome-like structure in C2C12 during myoblast fusion.

(A) C2C12 cells were cotransfected with EGFP-NRIP (green) and mCherry-actin (red) by K2 Transfection kit for 24 hr and shifted to differentiation medium for 24 hr, then

trypsinized and replated on Matrigel-coated cover glass and subjected to time-lapse microscopy. White arrows indicate the actin and NRIP foci. EGFP-NRIP and mCherry-actin colocalized and concentrated in cytoplasm to form actin and NRIP-enriched foci (0-30 min), and the foci protruded from cytoplasm toward cell membrane to form podosome-like structure (60-180 min) which may participate in myoblast fusion. Scale bar: 20 μ m.



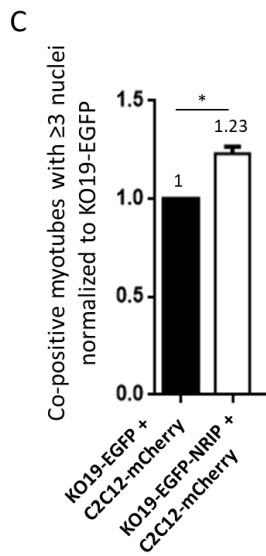
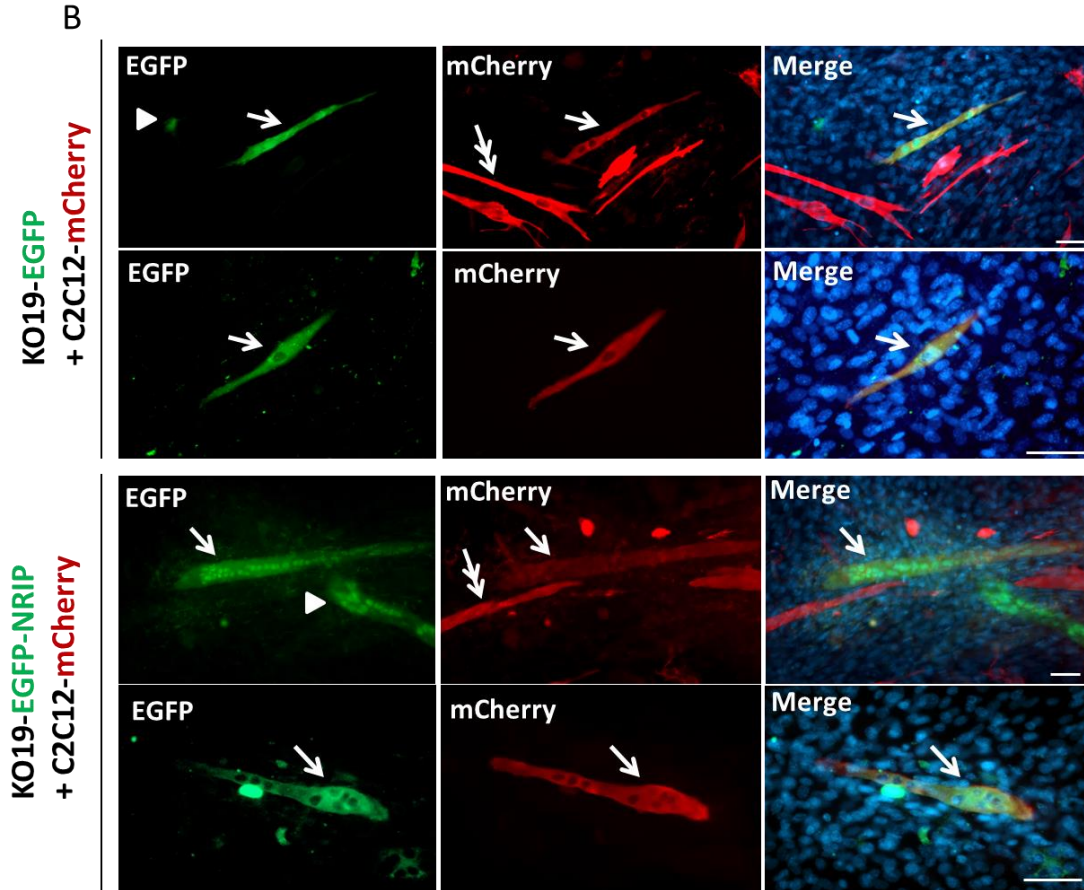
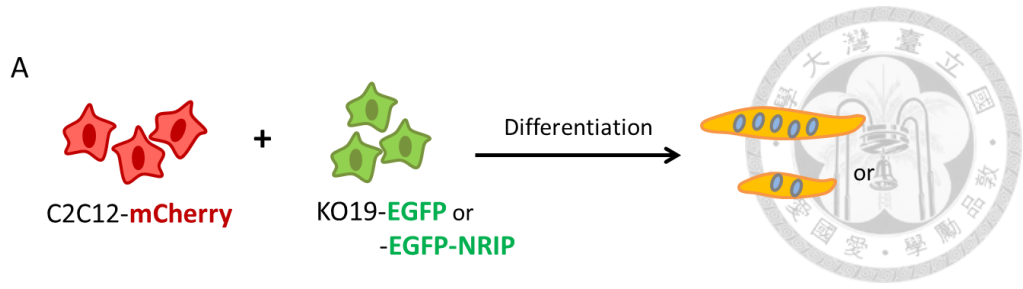


Figure 8. NRIP promotes myoblast fusion.

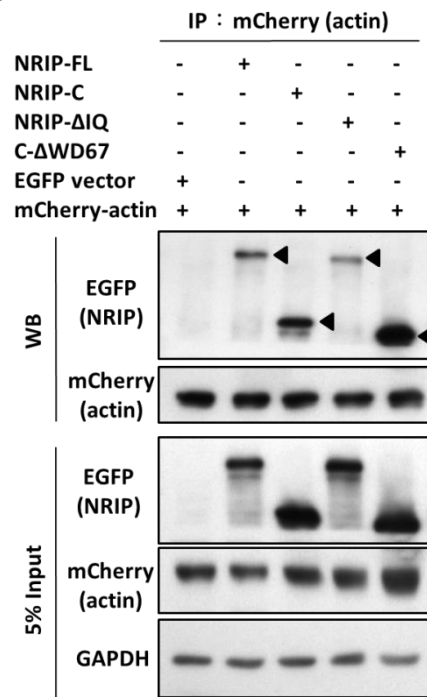
(A) The schematic illustration of cell fusion assay. C2C12 cells were transfected with mCherry vector to have red color; and KO19 cells (NRIP-null) were transfected with EGFP vector as control group or EGFP-NRIP as experimental group, and displayed green color, respectively. Then, C2C12 and KO19 were mixed together in a ratio of 1 to 1 (each cell line: 0.71×10^5 cells/ cm^2), and shifted to differentiation medium for 12 days to form myotubes. (B) NRIP is responsible for myotube formation. The mixed cells were stained with anti-EGFP and anti-DsRed for mCherry to enhance the fluorescence intensity after differentiation either EGFP⁺ (arrowhead) or mCherry⁺ (double-headed arrow) and co-positive cells (arrow). White arrow indicates the fused myotubes which express both EGFP and mCherry at the same time. KO19/EGFP-NRIP showed larger fused myotubes with more myonuclei than KO19/EGFP. Scale bar: 100 μm . (C) Quantitative analysis. Statistical analysis was calculated as the number of co-positive myotubes with three or more nuclei to the total number of co-positive myotubes. KO19/EGFP-NRIP had more myotubes with at least three nuclei than KO19/EGFP (KO19/EGFP set as 1; 1.23 vs. 1, $P < 0.05$). N=3, data are presented as mean \pm SEM. * $p < 0.05$; Student's t-test.



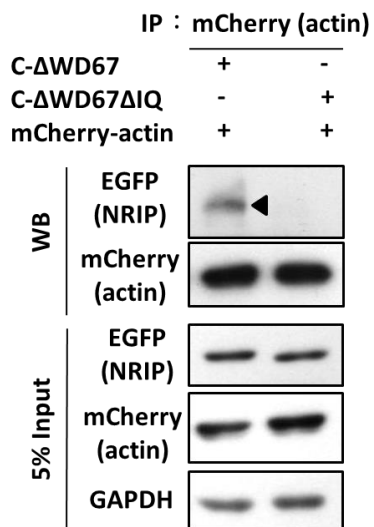
A



B



C



D

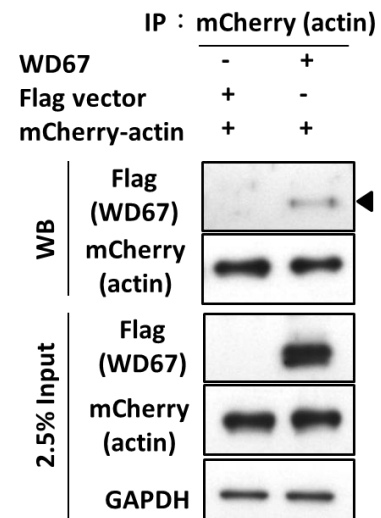


Figure 9. NRIP interacts with actin through WD67 domains.

(A) The schematic illustration of NRIP truncated mutants used for immunoprecipitation assay. NRIP-FL (Full length containing WD1-7 repeats and one IQ motif), NRIP- Δ IQ (containing WD1-7 domains without IQ motif), NRIP-C (containing WD67 domains and one IQ motif), C- Δ WD67 (containing one IQ motif), C- Δ WD67 Δ IQ (C-terminus without WD67 domains and IQ domain) are with EGFP tags, and WD67 (containing WD67 domains) is Flag-tagged. 293T cells were transiently co-transfected with each NRIP truncated mutant and mCherry-actin plasmids. Cell lysates were extracted and immunoprecipitated with anti-DsRed antibody for the detection of mCherry-actin. (B) NRIP may directly or indirectly interact with actin. Four NRIP truncated mutants, including NRIP-FL, NRIP- Δ IQ, NRIP-C and C- Δ WD67 could be detected by immunoprecipitation of mCherry-actin. EGFP vector was used as a negative control. Black arrows indicate the actin precipitated NRIP. (C) Either IQ domain or WD40 domain of NRIP is responsible for actin binding. There was no C- Δ WD67 Δ IQ precipitated by actin. (D) The WD67 domains of NRIP can interact with actin. WD67 could be detected by immunoprecipitation of mCherry-actin, indicating that WD67 domains of NRIP may be responsible for binding with actin. Flag vector was used as a negative control.

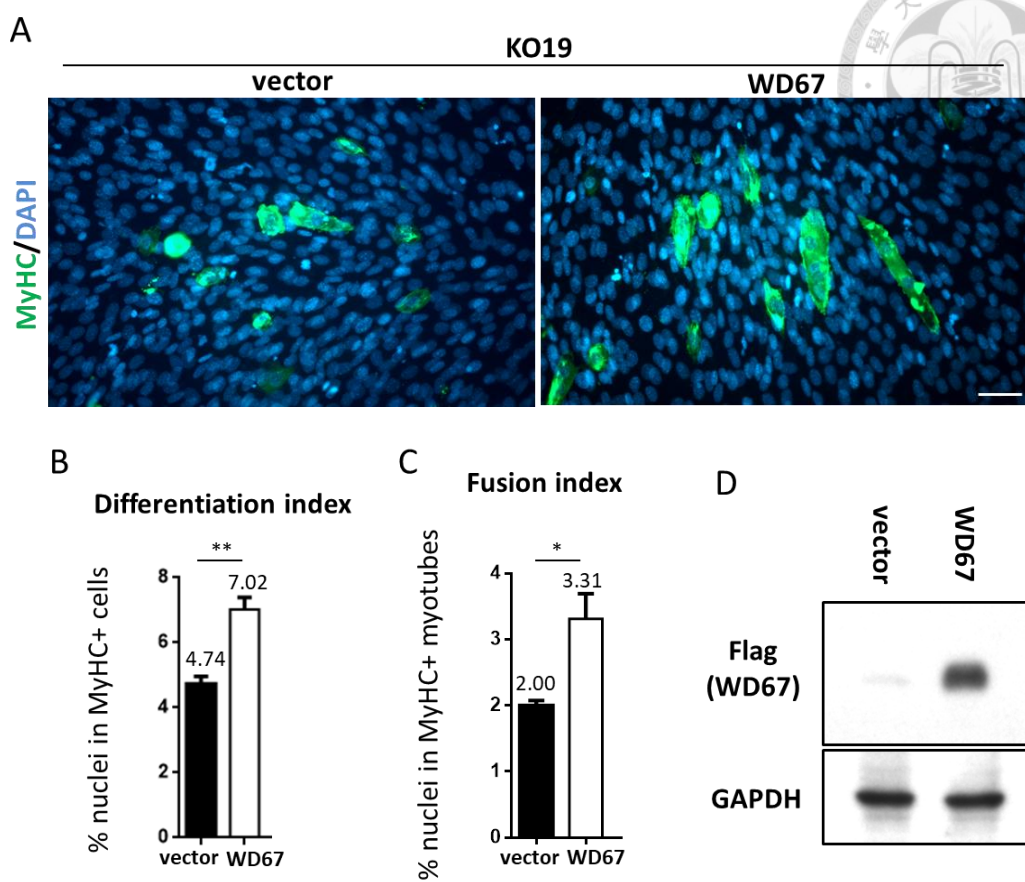


Figure 10. The WD67 domains of NRIP are related to myotube formation.

(A) KO19 cells were transfected with Flag-vector or Flag-WD67 plasmid for 24 hr and shifted to differentiation medium for 8 days, then stained with anti-myosin heavy chain (MyHC) antibody (green) and DAPI for nucleus (blue) to examine myotube formation, scale bar: 100 μ m. (B, C) Differentiation and fusion index were calculated as shown in Figure 3 (C, D). (B) Quantitative result. Differentiation index was significantly higher in KO19/WD67 than KO19/vector (7.02% vs. 4.74%, $P < 0.01$) (C) Fusion index was significantly increased in KO19/WD67 group compared to KO19/vector (3.31% vs. 2.00%, $P < 0.05$). $N = 3$, data are presented as mean \pm SEM. * $p < 0.05$ and ** $p < 0.01$; Student's t-test. (D) The protein expression of Flag-WD67 in KO19 cells transfected by K2 Transfection kit and detected by western blot.

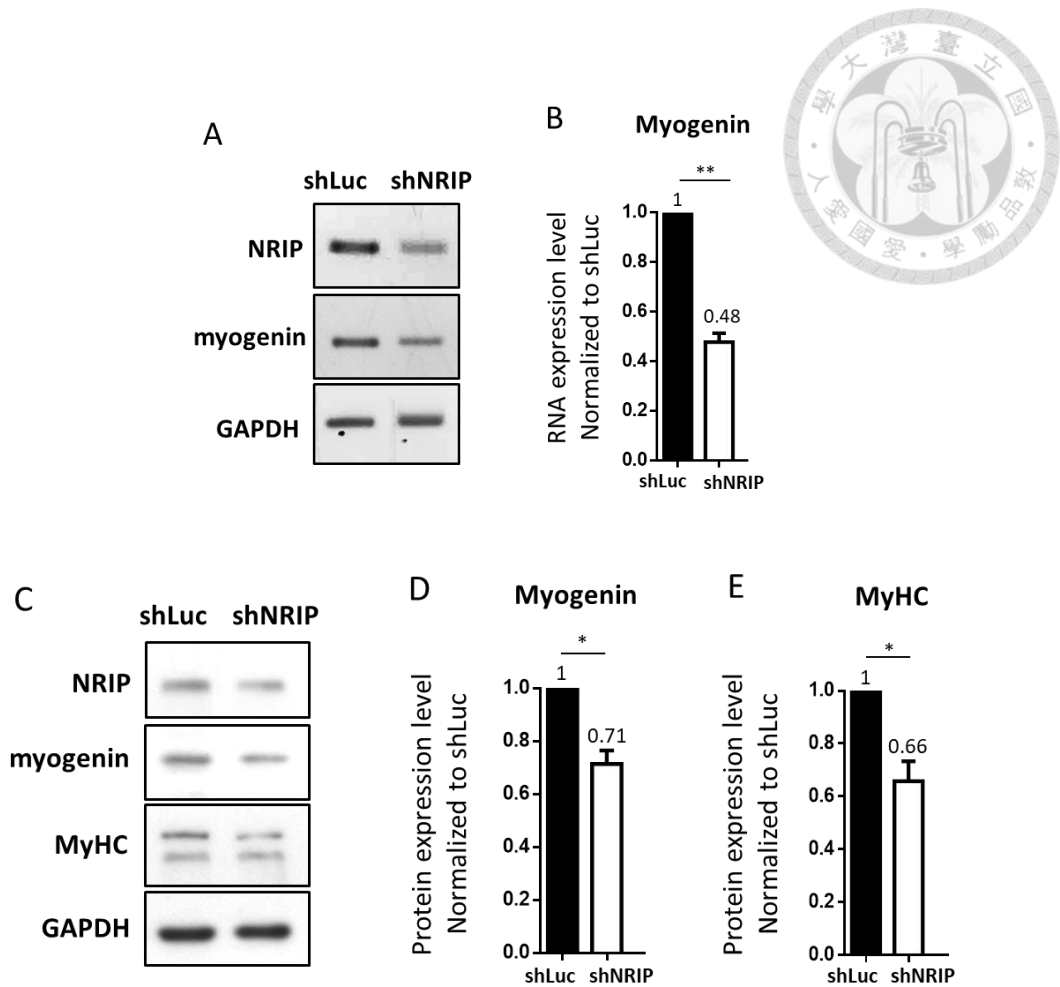


Figure 11. Knockdown of NRIP down-regulates the RNA and protein expression levels of myogenin and MyHC during C2C12 differentiation.

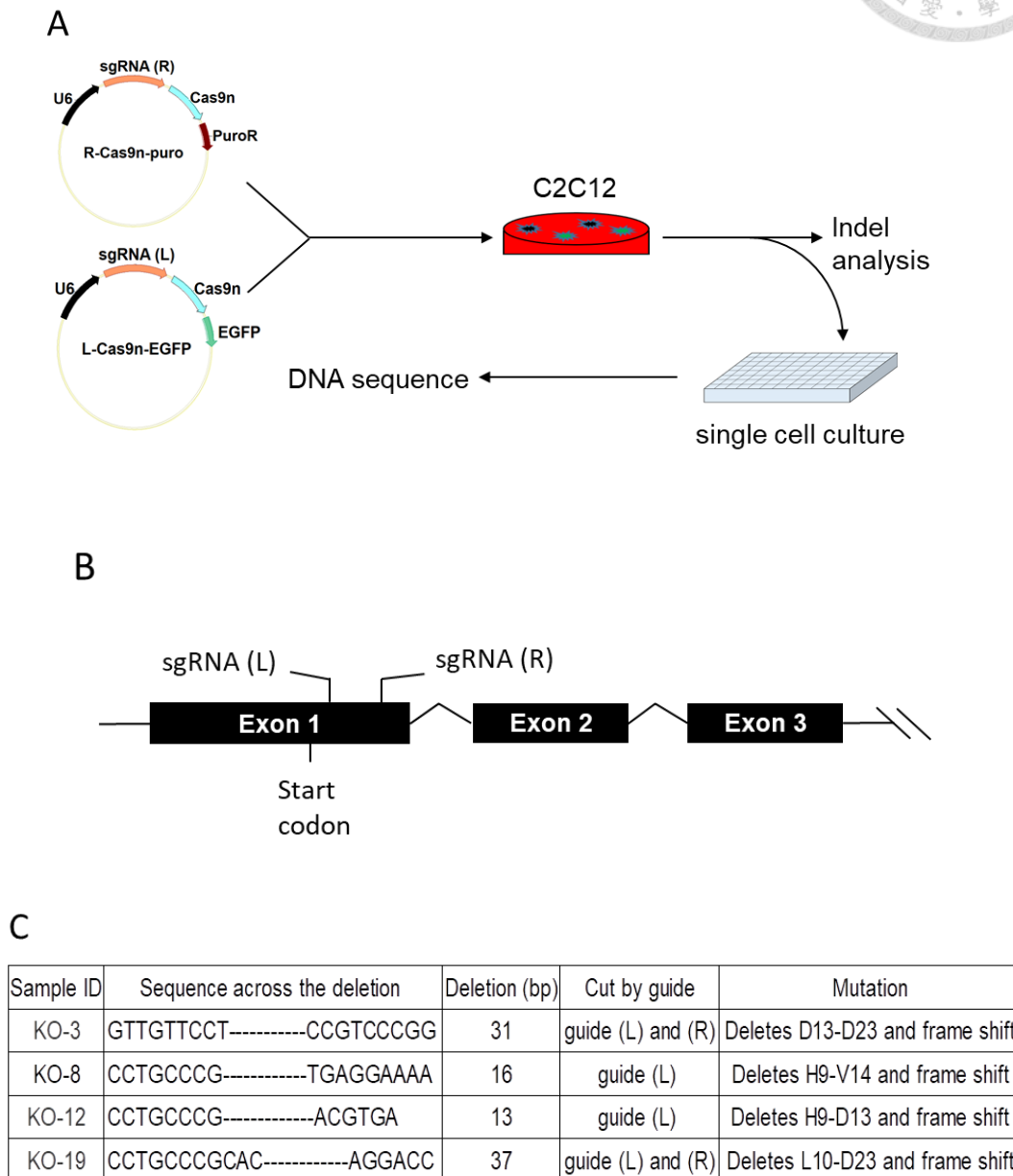
(A) PCR analysis of NRIP knockdown C2C12. C2C12 cells were differentiated for 3 days, and infected with adenovirus encoding shNRIP (named Ad-shNRIP, MOI=10 (Chen et al., 2018) for 2 days. RNA was extracted and analyzed by indicated primers (NRIP: forward 5'-TGG AAG AGC TGG ATA CTT TGA ACA, reverse 5'-AGT TGC GGT GGC CCT TAT AAA; myogenin: forward 5'-GCT GTA TGA AAC ATC CCC CTA, reverse 5'-CGC TGT GGG AGT TGC ATT) for RT-PCR and detected by agarose gel. (B) Quantitative result. The RNA expression level of myogenin was significantly reduced in Ad-shNRIP infected C2C12 than Ad-shLuc group (shLuc set as 1; shNRIP 0.48, $P < 0.01$). N=3. (C) Western blot analysis of NRIP knockdown C2C12. C2C12 cells were differentiated for 3 days, and infected with Ad-shNRIP (MOI=10) for 2 days. Cell lysates were extracted and detected by western blot. (D) Quantitative result showed that the protein expression level of myogenin was significantly decreased in shNRIP group than shLuc group (shLuc set as 1; shNRIP 0.71, $P < 0.05$) (E) Quantitative result. The protein expression level of MyHC was significantly lower in C2C12 infected with shNRIP than shLuc group. (shLuc set as 1; shNRIP 0.66, $P < 0.05$). N=4, data are

presented as mean \pm SEM. * p <0.05 and ** p <0.01; Student's t-test.



Chapter 6

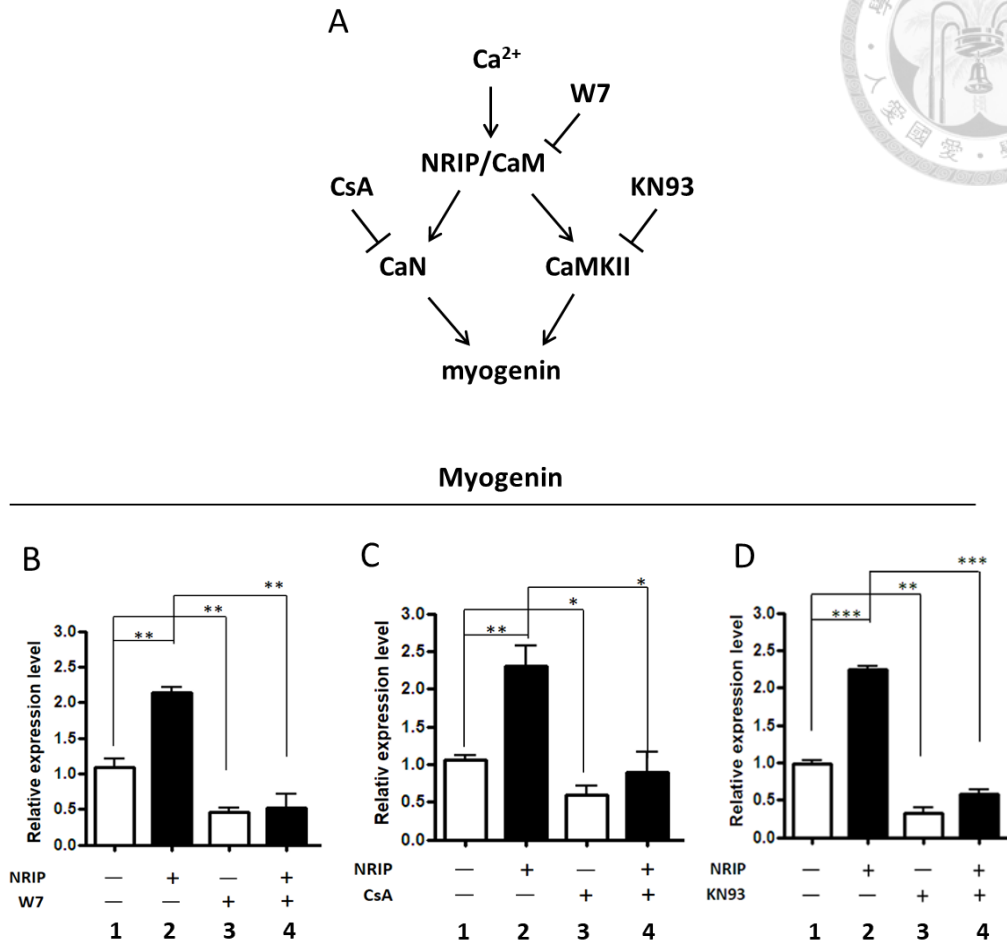
Supplementary information



Supplementary figure 1. Generation of NRIP-knockout C2C12 myoblasts—KO19 by CRISPR/Cas9 system (Hsin-Hsiung Chen's unpublished results).

(A) The schematic illustration of CRISPR for NRIP-knockout C2C12—KO19 myoblasts. Trypsinized C2C12 cells (1×10^5 cells) were added with $2 \mu\text{g}$ plasmids (sgRNA-L-Cas9n-EGFP:sgRNA-R-Cas9n-puro=3:1) and subjected to electroporation (1650 v/10 ms/3 pulses). The cells were seeded into 24-well plate containing antibiotic-free complete medium, and incubated overnight, followed by selected with

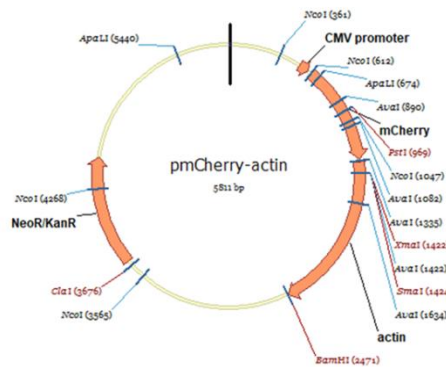
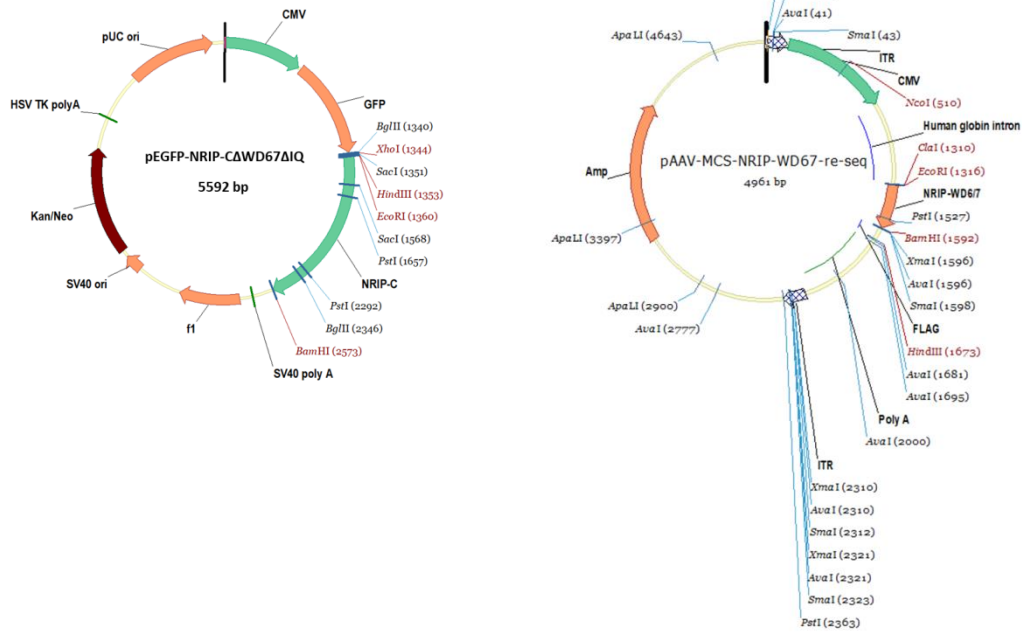
3 μ g/ml puromycin for 2 days, and harvested. Remaining cells were diluted to 0.5 cell per well and added into 96-well plate for single cell cultured for one month. Half of cells in each well were purified the genomic DNA to verify the DNA sequence. (B) The location of sgRNAs for NRIP gene editing. The NRIP gene consists of 19 exons with the translation start site at exon 1. The pair of sgRNAs target the NRIP exon 1 resulting frameshift mutation for NRIP deletion. (C) Sequencing of genomic PCR fragments from C2C12 cells following disruption of NRIP by CRISPR.



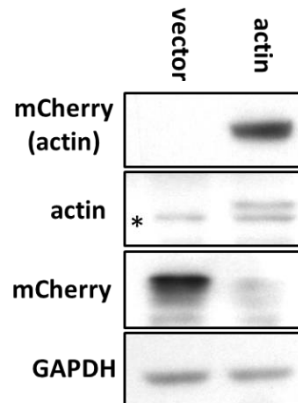
Supplementary figure 2. NRIP promotes myogenin expression through CaM signaling pathway (Hsin-Hsiung Chen's unpublished results).

(A) Working model. In the presence of Ca^{2+} , NRIP promotes myogenin expression through binding with CaM to activate CaN and CaMKII signaling pathway. W7 is a CaM inhibitor; cyclosporine A (CsA) is a calcineurin inhibitor and KN93 is a CaMKII inhibitor, respectively. (B) RT-qPCR analysis of myogenin expression with CaM inhibitor (W7) in C2C12. C2C12 cells were infected with Ad-NRIP or Ad-GFP (MOI=10) for 2 days and shifted to differentiation medium with the supplement of W7 (1 μ g/ml) or DMSO for 24 hours. NRIP-induced myogenin expression is inhibited by CaM inhibitor (W7). (C) Quantitative results. NRIP-induced RNA expression level of myogenin is inhibited by CaN inhibitor (CsA) (D) Quantitative results. NRIP-induced RNA expression level of myogenin is inhibited by CaMKII inhibitor (KN93). Data are presented by mean \pm SEM. * $p < 0.05$, ** $p < 0.01$ and *** $p < 0.001$; One-way ANOVA.

A

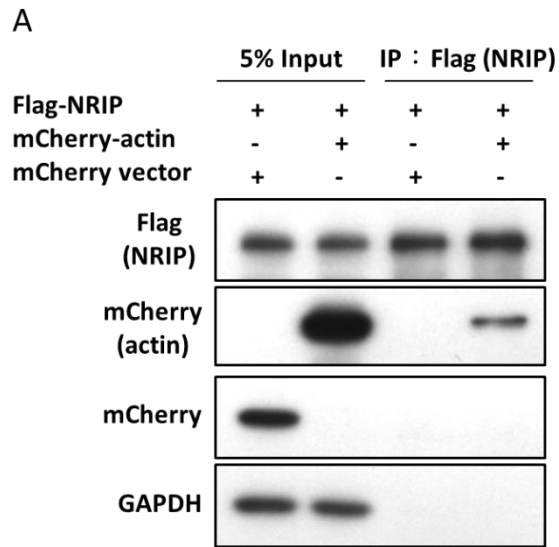


B



Supplementary figure 3. Maps of pEGFP-NRIP-CΔWD67ΔIQ, pAAV-NRIP-WD67, pmCherry-actin.

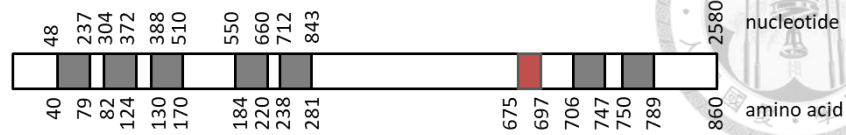
(A) Plasmid maps. pEGFP-NRIP-CΔWD67ΔIQ was cloned by using PCR-based site-directed mutagenesis. pEGFP-NRIP-CΔWD67 was used as template to amplified the target product with indicated primers: forward 5'-GAA TTG GAT ACT TTG AAC ATT AGA CC, reverse 5'-ATC ACC AGG TCC TGC TCG AT to delete IQ motif on pEGFP-NRIP-CΔWD67. The product was then treated with kinase, ligase and Dpn1 to ligate linear DNA into plasmid and remove template, followed by transforming into competent cells. (B) The protein expression of mCherry-actin in 293T cells transfected by jetPRIME. mCherry-actin was detected by anti-DsRed (for mCherry) and anti-actin antibodies. Asterisk indicates non-specific band.



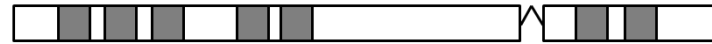
Supplementary figure 4. The immunoprecipitation assay of Flag-NRIP and mCherry-actin. (A) The same figure as Figure 1A, the mCherry band only presented in the input part, showing that there was no non-specific binding between Flag-NRIP and mCherry.

A

NRIP-FL



NRIP- Δ IQ



NRIP-C



C- Δ WD67



C- Δ WD67 Δ IQ



Supplementary figure 5. The schematic illustration of NRIP truncated mutants with nucleotide and amino acid numbers.

Chapter 7

Appendix

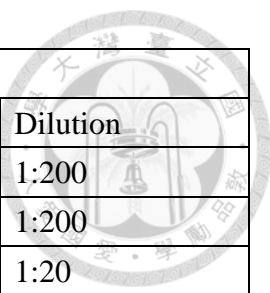


Guide RNA sequences for NRIP genome targeting	
Primer name	Primer sequences (5' to 3')
NRIP-sgRNA-F	GCC CGC ACC UGU UGU GGG AC
NRIP-sgRNA-R	CUU GGG CUG GAG GAC CCG UCC
Primers for pEGFP-NRIP-CΔWD67ΔIQ construction	
Primer name	Primer sequences (5' to 3')
EGFP-NRIP-C Δ WD67 Δ IQ-F	GAATTGGATACTTTGAACATTAGACC
EGFP-NRIP-C Δ WD67 Δ IQ-R	ATCACCAGGTCCTGCTCGAT

Appendix figure 1. Primer sequences.

Plasmid name	Plasmid backbone
Flag-NRIP	p3xFLAG-CMV-14
mCherry-actin	pmCherry-C1
NRIP-FL	pEGFP-N1
NRIP- Δ IQ	pEGFP-N1
NRIP-C	pEGFP-N1
C- Δ WD67	pEGFP-N1
C- Δ WD67 Δ IQ	pEGFP-N1
WD67	pAAV-MCS
L-Cas9n-EGFP	pSpCas9n(BB)-2A-GFP
R-Cas9n-puro	pSpCas9n(BB)-2A-Puro

Appendix figure 2. Plasmid backbones list.



Cell staining			
Antibody name	Company	Cat NO.	Dilution
NRIP	GeneTex	GTX105954	1:200
Heavy chain myosin	Abcam	ab124205	1:200
GFP	Santa Cruz	sc-9996	1:20
mCherry	TaKaRa	632496	1:200
Western Blot			
Antibody name	Company	Cat NO.	Dilution
NRIP	Novus	NBP1-30075	1:2000
Myogenin	Santa Cruz	sc-12732	1:2000
Heavy chain myosin	Abcam	ab124205	1:2000
Flag	Abcam	Ab1162	1:10000
GFP	Abcam	ab183734	1:10000
GAPDH	AbFrontier	LF-PA0212	1:10000
EGF receptor	Cell Signaling	C74B9	1:1000

Appendix figure 3. Primary antibodies list.

Chapter 8

References



Abmayr, S.M., and Pavlath, G.K. (2012). Myoblast fusion: lessons from flies and mice. *Development* *139*, 641-656.

Abraham, S.T., and Shaw, C. (2006). Increased expression of deltaCaMKII isoforms in skeletal muscle regeneration: Implications in dystrophic muscle disease. *J Cell Biochem* *97*, 621-632.

Appleton, B.A., Wu, P., and Wiesmann, C. (2006). The crystal structure of murine coronin-1: a regulator of actin cytoskeletal dynamics in lymphocytes. *Structure* *14*, 87-96.

Bahler, M., and Rhoads, A. (2002). Calmodulin signaling via the IQ motif. *FEBS Lett* *513*, 107-113.

Bassel-Duby, R., and Olson, E.N. (2006). Signaling pathways in skeletal muscle remodeling. *Annu Rev Biochem* *75*, 19-37.

Bentzinger, C.F., Wang, Y.X., and Rudnicki, M.A. (2012). Building muscle: molecular regulation of myogenesis. *Cold Spring Harb Perspect Biol* *4*.

Berger, S., Schafer, G., Kesper, D.A., Holz, A., Eriksson, T., Palmer, R.H., Beck, L., Klambt, C., Renkawitz-Pohl, R., and Onel, S.F. (2008). WASP and SCAR have distinct roles in activating the Arp2/3 complex during myoblast fusion. *Journal of Cell Science* *121*, 1303-1313.

Berkes, C.A., and Tapscott, S.J. (2005). MyoD and the transcriptional control of myogenesis. *Semin Cell Dev Biol* *16*, 585-595.

Bernadzki, K.M., Rojek, K.O., and Proszynski, T.J. (2014). Podosomes in muscle cells and their role in the remodeling of neuromuscular postsynaptic machinery. *Eur J Cell Biol* *93*, 478-485.

Bi, P., Ramirez-Martinez, A., Li, H., Cannavino, J., McAnally, J.R., Shelton, J.M., Sanchez-Ortiz, E., Bassel-Duby, R., and Olson, E.N. (2017). Control of muscle

formation by the fusogenic micropeptide myomixer. *Science* 356, 323-327.

Bogdan, S., and Klambt, C. (2003). Kette regulates actin dynamics and genetically interacts with Wave and Wasp. *Development* 130, 4427-4437.

Chal, J., and Pourquie, O. (2017). Making muscle: skeletal myogenesis in vivo and in vitro. *Development* 144, 2104-2122.

Chang, S.W., Tsao, Y.P., Lin, C.Y., and Chen, S.L. (2011). NRIP, a novel calmodulin binding protein, activates calcineurin to dephosphorylate human papillomavirus E2 protein. *J Virol* 85, 6750-6763.

Chen, E.H. (2011). Invasive podosomes and myoblast fusion. *Curr Top Membr* 68, 235-258.

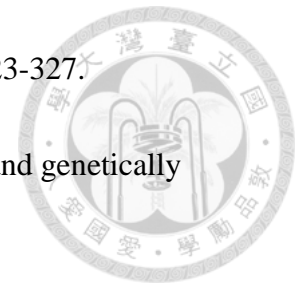
Chen, E.H., and Olson, E.N. (2004). Towards a molecular pathway for myoblast fusion in *Drosophila*. *Trends Cell Biol* 14, 452-460.

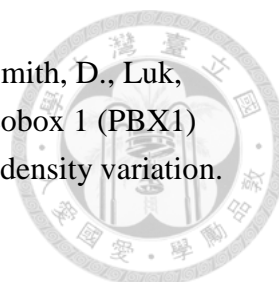
Chen, H.H., Chen, W.P., Yan, W.L., Huang, Y.C., Chang, S.W., Fu, W.M., Su, M.J., Yu, I.S., Tsai, T.C., Yan, Y.T., *et al.* (2015). NRIP is newly identified as a Z-disc protein, activating calmodulin signaling for skeletal muscle contraction and regeneration. *J Cell Sci* 128, 4196-4209.

Chen, H.H., Fan, P., Chang, S.W., Tsao, Y.P., Huang, H.P., and Chen, S.L. (2017). NRIP/DCAF6 stabilizes the androgen receptor protein by displacing DDB2 from the CUL4A-DDB1 E3 ligase complex in prostate cancer. *Oncotarget* 8, 21501-21515.

Chen, H.H., Tsai, L.K., Liao, K.Y., Wu, T.C., Huang, Y.H., Huang, Y.C., Chang, S.W., Wang, P.Y., Tsao, Y.P., and Chen, S.L. (2018). Muscle-restricted nuclear receptor interaction protein knockout causes motor neuron degeneration through down-regulation of myogenin at the neuromuscular junction. *J Cachexia Sarcopenia Muscle* 9, 771-785.

Chen, P.H., Tsao, Y.P., Wang, C.C., and Chen, S.L. (2008). Nuclear receptor interaction protein, a coactivator of androgen receptors (AR), is regulated by AR and Sp1 to feed forward and activate its own gene expression through AR protein stability. *Nucleic Acids Res* 36, 51-66.





Cheung, C.L., Chan, B.Y., Chan, V., Ikegawa, S., Kou, I., Ngai, H., Smith, D., Luk, K.D., Huang, Q.Y., Mori, S., *et al.* (2009). Pre-B-cell leukemia homeobox 1 (PBX1) shows functional and possible genetic association with bone mineral density variation. *Hum Mol Genet* 18, 679-687.

Chuang, M.C., Lin, S.S., Ohniwa, R.L., Lee, G.H., Su, Y.A., Chang, Y.C., Tang, M.J., and Liu, Y.W. (2019). Tks5 and Dynamin-2 enhance actin bundle rigidity in invadosomes to promote myoblast fusion. *J Cell Biol* 218, 1670-1685.

Dalkilic, I., Schienda, J., Thompson, T.G., and Kunkel, L.M. (2006). Loss of FilaminC (FLNc) results in severe defects in myogenesis and myotube structure. *Mol Cell Biol* 26, 6522-6534.

Demonbreun, A.R., Lapidos, K.A., Heretis, K., Levin, S., Dale, R., Pytel, P., Svensson, E.C., and McNally, E.M. (2010). Myoferlin regulation by NFAT in muscle injury, regeneration and repair. *J Cell Sci* 123, 2413-2422.

Dominguez, R., and Holmes, K.C. (2011). Actin structure and function. *Annu Rev Biophys* 40, 169-186.

Ehret, G.B., O'Connor, A.A., Weder, A., Cooper, R.S., and Chakravarti, A. (2009). Follow-up of a major linkage peak on chromosome 1 reveals suggestive QTLs associated with essential hypertension: GenNet study. *Eur J Hum Genet* 17, 1650-1657.

Friday, B.B., Mitchell, P.O., Kegley, K.M., and Pavlath, G.K. (2003). Calcineurin initiates skeletal muscle differentiation by activating MEF2 and MyoD. *Differentiation* 71, 217-227.

Ganassi, M., Badodi, S., Ortuste Quiroga, H.P., Zammit, P.S., Hinitis, Y., and Hughes, S.M. (2018). Myogenin promotes myocyte fusion to balance fibre number and size. *Nat Commun* 9, 4232.

Hamoud, N., Tran, V., Croteau, L.P., Kania, A., and Cote, J.F. (2014). G-protein coupled receptor BAI3 promotes myoblast fusion in vertebrates. *Proc Natl Acad Sci U S A* 111, 3745-3750.

Han, C.P., Lee, M.Y., Tzeng, S.L., Yao, C.C., Wang, P.H., Cheng, Y.W., Chen, S.L., Wu, T.S., Tyan, Y.S., and Kok, L.F. (2008). Nuclear Receptor Interaction Protein (NRIP)

expression assay using human tissue microarray and immunohistochemistry technology confirming nuclear localization. *J Exp Clin Cancer Res* 27, 25.

Hartwig, J.H., and Stossel, T.P. (1975). Isolation and properties of actin, myosin, and a new actinbinding protein in rabbit alveolar macrophages. *J Biol Chem* 250, 5696-5705.

Hochreiter-Hufford, A.E., Lee, C.S., Kinchen, J.M., Sokolowski, J.D., Arandjelovic, S., Call, J.A., Klibanov, A.L., Yan, Z., Mandell, J.W., and Ravichandran, K.S. (2013). Phosphatidylserine receptor BAI1 and apoptotic cells as new promoters of myoblast fusion. *Nature* 497, 263-267.

Kang, J.S., and Krauss, R.S. (2010). Muscle stem cells in developmental and regenerative myogenesis. *Curr Opin Clin Nutr Metab Care* 13, 243-248.

Kim, J.H., Jin, P., Duan, R., and Chen, E.H. (2015). Mechanisms of myoblast fusion during muscle development. *Curr Opin Genet Dev* 32, 162-170.

Kim, S., Shilagardi, K., Zhang, S., Hong, S.N., Sens, K.L., Bo, J., Gonzalez, G.A., and Chen, E.H. (2007). A critical function for the actin cytoskeleton in targeted exocytosis of pre-fusion vesicles during myoblast fusion. *Dev Cell* 12, 571-586.

Knight, J.D., and Kothary, R. (2011). The myogenic kinome: protein kinases critical to mammalian skeletal myogenesis. *Skelet Muscle* 1, 29.

Li, D., and Roberts, R. (2001). WD-repeat proteins: structure characteristics, biological function, and their involvement in human diseases. *Cell Mol Life Sci* 58, 2085-2097.

Millay, D.P., O'Rourke, J.R., Sutherland, L.B., Bezprozvannaya, S., Shelton, J.M., Bassel-Duby, R., and Olson, E.N. (2013). Myomaker is a membrane activator of myoblast fusion and muscle formation. *Nature* 499, 301-305.

Millay, D.P., Sutherland, L.B., Bassel-Duby, R., and Olson, E.N. (2014). Myomaker is essential for muscle regeneration. *Gene Dev* 28, 1641-1646.

Mimura, N., and Asano, A. (1986). Isolation and characterization of a conserved actin-binding domain from rat hepatic actinogelin, rat skeletal muscle, and chicken gizzard alpha-actinins. *J Biol Chem* 261, 10680-10687.

Nowak, S.J., Nahirney, P.C., Hadjantonakis, A.K., and Baylies, M.K. (2009). Nap1-mediated actin remodeling is essential for mammalian myoblast fusion. *J Cell Sci* 122, 3282-3293.

Oku, T., Itoh, S., Okano, M., Suzuki, A., Suzuki, K., Nakajin, S., Tsuji, T., Nauseef, W.M., and Toyoshima, S. (2003). Two regions responsible for the actin binding of p57, a mammalian coronin family actin-binding protein. *Biol Pharm Bull* 26, 409-416.

Park, S.Y., Yun, Y., Lim, J.S., Kim, M.J., Kim, S.Y., Kim, J.E., and Kim, I.S. (2016). Stabilin-2 modulates the efficiency of myoblast fusion during myogenic differentiation and muscle regeneration. *Nat Commun* 7, 10871.

Powell, G.T., and Wright, G.J. (2012). Do muscle founder cells exist in vertebrates? *Trends in Cell Biology* 22, 391-396.

Quinn, M.E., Goh, Q., Kurosaka, M., Gamage, D.G., Petrany, M.J., Prasad, V., and Millay, D.P. (2017). Myomerger induces fusion of non-fusogenic cells and is required for skeletal muscle development. *Nat Commun* 8, 15665.

Richardson, B.E., Beckett, K., Nowak, S.J., and Baylies, M.K. (2007). SCAR/WAVE and Arp2/3 are crucial for cytoskeletal remodeling at the site of myoblast fusion. *Development* 134, 4357-4367.

Rodal, A.A., Tetreault, J.W., Lappalainen, P., Drubin, D.G., and Amberg, D.C. (1999). Aip1p interacts with cofilin to disassemble actin filaments. *J Cell Biol* 145, 1251-1264.

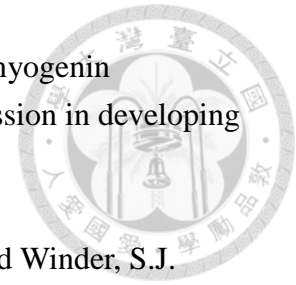
Sens, K.L., Zhang, S., Jin, P., Duan, R., Zhang, G., Luo, F., Parachini, L., and Chen, E.H. (2010). An invasive podosome-like structure promotes fusion pore formation during myoblast fusion. *J Cell Biol* 191, 1013-1027.

Shi, Y., Li, Z., Xu, Q., Wang, T., Li, T., Shen, J., Zhang, F., Chen, J., Zhou, G., Ji, W., *et al.* (2011). Common variants on 8p12 and 1q24.2 confer risk of schizophrenia. *Nat Genet* 43, 1224-1227.

Smith, T.F., Gaitatzes, C., Saxena, K., and Neer, E.J. (1999). The WD repeat: a common architecture for diverse functions. *Trends Biochem Sci* 24, 181-185.

Tang, H., Macpherson, P., Argetsinger, L.S., Cieslak, D., Suhr, S.T., Carter-Su, C., and

Goldman, D. (2004). CaM kinase II-dependent phosphorylation of myogenin contributes to activity-dependent suppression of nAChR gene expression in developing rat myotubes. *Cell Signal* 16, 551-563.



Thompson, O., Kleino, I., Crimaldi, L., Gimona, M., Saksela, K., and Winder, S.J. (2008). Dystroglycan, Tks5 and Src mediated assembly of podosomes in myoblasts. *PLoS One* 3, e3638.

Thompson, T.G., Chan, Y.M., Hack, A.A., Brosius, M., Rajala, M., Lidov, H.G., McNally, E.M., Watkins, S., and Kunkel, L.M. (2000). Filamin 2 (FLN2): A muscle-specific sarcoglycan interacting protein. *J Cell Biol* 148, 115-126.

Tixier, V., Bataille, L., and Jagla, K. (2010). Diversification of muscle types: recent insights from *Drosophila*. *Exp Cell Res* 316, 3019-3027.

Tsai, T.C., Lee, Y.L., Hsiao, W.C., Tsao, Y.P., and Chen, S.L. (2005). NRIP, a novel nuclear receptor interaction protein, enhances the transcriptional activity of nuclear receptors. *J Biol Chem* 280, 20000-20009.

van der Ven, P.F., Wiesner, S., Salmikangas, P., Auerbach, D., Himmel, M., Kempa, S., Hayess, K., Pacholsky, D., Taivainen, A., Schroder, R., *et al.* (2000). Indications for a novel muscular dystrophy pathway. gamma-filamin, the muscle-specific filamin isoform, interacts with myotilin. *J Cell Biol* 151, 235-248.

Voegtli, W.C., Madrona, A.Y., and Wilson, D.K. (2003). The structure of Aip1p, a WD repeat protein that regulates Cofilin-mediated actin depolymerization. *J Biol Chem* 278, 34373-34379.

Welch, M.D., DePace, A.H., Verma, S., Iwamatsu, A., and Mitchison, T.J. (1997). The human Arp2/3 complex is composed of evolutionarily conserved subunits and is localized to cellular regions of dynamic actin filament assembly. *Journal of Cell Biology* 138, 375-384.

Zhang, Q., Vashisht, A.A., O'Rourke, J., Corbel, S.Y., Moran, R., Romero, A., Miraglia, L., Zhang, J., Durrant, E., Schmedt, C., *et al.* (2017). The microprotein Minion controls cell fusion and muscle formation. *Nat Commun* 8, 15664.

Zhang, Y., Ye, J.W., Chen, D.Z., Zhao, X.Y., Xiao, X.J., Tai, S., Yang, W., and Zhu, D.H.

(2006). Differential expression profiling between the relative normal and dystrophic muscle tissues from the same LGMD patient. *J Transl Med* 4.

